Republic of Iraq

Ministry of Higher Education and Scientific

Research University of Babylon

College of Engineering

Design and Fabrication of Microstrip Patch Antenna based on Carbon Nanotube

A Thesis

Submitted to the College of Engineering / University of Babylon in Partial Fulfillment of the Requirements for the Degree of Master of Science in Engineering / Electrical Engineering /Industrial Electronic

By

Saif Hilal Zedan Noori

Supervised by

Dr. Haider Al- Mumen

2022 A.D **1444 A.H**

بسْمِ ا لَلهِّ الرحْمَنِ الرحِيمِ

﴿ نَرْفَعُ دَرَجَاتٍ مَنْ نَشَاءُ وَفَوْقَ كُلِّ ذِي عِلْمٍ عَلِيمٌ ﴾

(صدقَ اللّه الْعَلي الْعَظِيم)

سورة يوسف/ الآية (76)

Supervisor certification

I certify that the thesis entitled **"Design and Fabrication of Microstrip Patch Antenna based on Carbon Nanotube"** was prepared by **Saif Hilal Zedan** under my supervision at the department of electrical engineering, college of engineering, university of Babylon, as partial fulfillment of requirements for the degree of master in engineering /electrical engineering/industrial electronic.

Supervisor

Signature:

Name :**Asst. Prof. Dr.Haider Sahib Al-Mumen**

Date: / / 2022

In view of the above recommendation, I am forward this thesis for discussion by the Examination Committee.

Head of Electrical Engineering Department

Signature:

Name: **Asst. Prof. Dr. Shamam Fadhil Alwash**

Date**:** / / 2022

Examining Committee Certificate

We certify that we have read this thesis entitled **"Design and Fabrication of Microstrip Patch Antenna based on Carbon Nanotube"** and as an examining committee examined the student **Saif Hilal Zedan** in its content and that in our opinion it meets a standard of a thesis for the degree of master in engineering/electrical engineering/ industrial electronic.

Signature:
Name: **Prof.**
Dr. Saad Saffah Hasson
(Chairman)
Date: / /2022

Signature:
Name: **Dr. Mohammed Taih Gatte**
(Member)
Date: / /2022

Signature:
Name: **Asst. Prof.**
Dr. Ahmed Mohammed Al-Hilli
(Member)
Date: / /2022

Signature:
Name: **Asst. Prof.**
Dr.Haider Sahib Al-Mumen
(Supervisor)
Date: / /2022

Signature:
Name: **Prof.**
Dr. Hatem Hadi Obeid
(Dean of College Of Engineering)
Date: / /2022

Signature:
Name: **Asst. Prof.**
Dr. Shamam Fadhil Alwash
(Head of Electrical Department)
Date: / /2022

Acknowledgment

First, I would like to thank my parents, wife, brothers and friends for providing support and encouragement throughout the work on this thesis.

I would also like to thank my supervisor, Dr. Haider Al- Mumen , who has inspired me throughout my research work and provided effective advice in critical times.

I would also like to thank the Electrical Engineering Department in particular and the College of Engineering in general for providing all the requirements to complete this thesis.

ABSTRACT

As a result of the development of wireless communication systems and keeping pace with modern technology, which requires antennas that are easy to manufacture and characterized by their high performance despite their small size and low cost. Therefore, the microstrip patch antenna (MPA) has been discussed that used in many applications at high frequencies.

The objective of this thesis is to design and to implement rectangular MPA based on copper and Carbon nanotube (CNT) that operate within the radio frequency range. The MPA designed using CST software version 18.0. First, copper used as a radiating patch, then CNT used instead of copper. In both cases, the same materials used to design the MPA. A substrate of Flame retardant 4 (FR4) with ε_r = 4.3 and h = 1.6 mm was used and the ground of copper. The thickness of copper is 0.035 mm, which is the same thickness of carbon nanotube. A single patch antenna as well as an array of patches were designed and simulated. The array consists of two and four elements of patches. It was designed using two different ways, series and parallel feeding lines. The characteristics of both copper and CNT patch antennas were analyzed. The operating frequency of all proposed antennas was 2.4 GHz, which is used for many applications including Wi-Fi and Bluetooth. The return loss of the designed antennas was less than -10 dB, while the voltage standing wave ratio (VSWR) was between 1 and 1.5. The properties of MPA including return loss, VSWR, gain, directivity, efficiency, radiation pattern were obtained at the resonant frequency.

Several microstrip patch antennas were fabricated using CNC machine and tested experimentally using Nano VNA instrument. Furthermore, a comparison was done to figure out the property difference between the fabricated and simulated antennas. In addition, a copper patch antennas coated with a CNT was fabricated and tested.

List of Contents

List of Abbreviations

Abbreviation	Definition
TL	Transmission Line
RL	Return Loss
VSWR	Voltage standing wave ratio
GEMS	General Electromagnetic Solver
FR4	Flame Retardant 4
HFSS	High Frequency Structural Simulator
CST MS	Computer Simulation Technology Microwave Studio
MPA	Microstrip Patch Antenna
R-MPA	Rectangular Microstrip Patch Antenna
CNT	Carbon Nanotube
SWCNT	Single walled carbon nanotube
MWCNT	Multi walled carbon nanotube
2D	Two Dimension
3D	Three Dimension
SEM	Scanning electron microscopy
PCB	Printed circuit board
CNC	computer numerical control
VNA	Vector network analyzer

List of Symbols

SYMBOL	Description
U	radiation intensity (W/unit solid angle)
W_{rad}	radiation density (w/m^2)
E	electric field
H	magnetic field
D	directivity (without units)
D_0	maximum directivity (without units)
U_{max}	intensity of maximum radiation (W/unit solid angle)
U_0	intensity of radiation of isotropic source (W/unit solid angle)
P_{rad}	total radiated power (W)
G	gain of antenna (without units)
K	antenna efficiency
G_{dB}	antenna gain in decibels
p	power
I	current
Rr	radiation resistance
p_r	radiated power from antenna
p_L	loss power
P_{tra}	transmitted power to antenna
P_{ref}	reflected power from antenna
Γ	reflection coefficient
f_H	upper frequency

f_L	lower frequency
f_c	center frequency
BW	bandwidth
(λo)	free-space wavelength
N	number of array elements
f_r	resonant (operating) frequency
h	thickness (height) of substrate
t	thickness (height) of patch = thickness (height) of ground
ε_r	dielectric constant of substrate
W	width of patch antenna
L	length of patch antenna
L_{eff}	effective length of patch
ϵ_{reff}	effective dielectric constant
ΔL	length extension
w_s	width of substrate = width of ground (w_g)
L_s	length of substrate = length of ground (L_g)
C	speed of light in space (C= 3×10^8 m/s)
W_f	feed line width
L_f	feed line length
Z_0	equivalent to feed line impedance
R_{in}	resonant input resistance
f_i	length of feed inset
G_{pf}	gap feed line spacing
dB	Decibels

List of Tables

List of Figures

Chapter One

Introduction

1.1 Introduction to antennas

For the wireless systems, an antenna is an essential component. The well design for the antenna can elevate the total system performance. The antenna can be defined as a device transmit or receive electromagnetic waves. In 1886, Hertz showed the first wireless electromagnetic system. In 1901, Marconi make good in transmitting signals through a wide distance from England to Newfoundland [1]. Antennas works proficiently over a comparatively narrow frequency range. The antenna should be seted to the like frequency range that the radio system to which it is linked, if not, the system of reception and transmission will be weaken. The transmitting antenna sending the electromagnetic wave by transmission line (TL) to the free space, on the other side the receiving antenna converts it into an electrical signal. The characteristics of the antennas are expressed by (Maxwell's equations). [2]

In this thesis, the studying of microstrip patch antenna was our interest , where its components and types are studied and analyzed. It is classified into several shapes. The rectangle was chosen for its design. we included nanomaterials in the field of design in addition to the commonly used metal material. After the success of designing the antennas by the program, we manufactured them experimentally to find out the possibility of compatibility between the proposed designs and the designs manufactured on the ground. The uses of the patch antenna are very important nowadays as it is designed to operate at high frequencies suitable for advanced devices in all technical, medical and other fields. The entry of nanomaterials into the formation of these antennas has a very effective role for their development, as nanomaterials have unique properties such as their high electrical and thermal conductivity, flexibility and ease of integration with many chemicals.

1.2 Microstrip Antenna

A microstrip patch antenna (MPA) consists of a conducting patch of any non-planar or planar geometry on one side of a dielectric substrate and a ground plane on other side. It is a printed resonant antenna for narrow-band microwave wireless links requiring semi-hemispherical coverage. Due to its planar configuration and ease of integration with microstrip technology, the MPA has been deeply. The rectangular and circular patches are the basic and most commonly used microstrip antennas [3].

The microstrip patch antennas are famous for their performance and robust design. MPA has applications in various fields such as in the medical field, satellites and even in the military systems just like in the rockets, aircrafts missiles and many more. Now it is booming in the commercial aspects due to their low cost of the substrate material and the fabrication. The technological advancement of the MPA is increasing day by day. A lot of research work is going on microstrip antenna for its better utilization in the future. Many techniques are coming into existence by compensating the gain and bandwidth of the MPA [3].

1.3 Literature Review

Kant and **D.C.Dhubkarya (2010),** designed and analyzed of (H-Shape) microstrip patch antenna by using IE3D software. They used an antenna operated at (2 GHz), they used cavity model to compare the simulation results with the practical results. They obtained the gain (11.3677dB_i) and directivity of (7.28714 dB_i**)** from the designed antenna [4]**.**

Patel and **Kosta (2011)**, designed (E-shape) MPA by using (HFSS) software. The range of frequency between (1200 to 1280 MHz) and these frequencies are useful for (GPS) applications. They used a coaxial probe feed to feeding the designed

antenna .The simulated results were showed the value of VSWR was less than two within the produced frequency band [5].

SANDEEP and **KASHYAP (2012)**, designed the rectangular microstrip patch array (2*2) antenna by using HFSS software to achieve gain of 11.6 dB at 2.4 GH_z .The different results were simulated to make a comparision with another frequency .The gain was 8 dB at 2.25 GHz [6].

Paul and **Sultan (2013),** simulated and analyzed the performance of the line feed rectangular patch antenna . They used the GEMS software to design and simulate the antenna at frequency 3 GHz. Their goal was studying effect of the dimensions (Length and Width) of the antenna and the parameters of the substrate (dielectric constant, thickness) on the properties of the radiation [7].

Casu et al **(2014)**, designed and implemented 4*1 and 8*1 patch antenna array using IE3D software**,** these antennas operate on a frequency 2.4 GHz . A dielectric material FR4 with dielectric substrate permittivity of 4.28 and height of 1.6 mm [8].

Çaliskan et al **(2015)**, designed a microstrip patch antenna for breast cancer detection operating at 2.45 GHz by using HFSS software. The substrate material is FR4 (ε_r = 4.4) [9].

Midasala and **Dr. P. Siddaiah (2016)**, designed 3*3 rectangular microstrip antenna array to improve better gains .In this research, they obtained a gain of 17.29 dB at frequency of 13 GHz by using HFSS 14.0 software. VSWR was 0.7807 [10].

Devi et al **(2017)**, fabricated multiwalled carbon nanotube(MWCNT) patch antenna to increase the bandwidth by 20% from the standard patch antenna made of copper with the same frequency. MWCNT ink was coating on FR4 sheet with

relative permittivity of 4.4. The gain was 8.3 dB for Standard copper patch antenna and it was 7 dB for MWCNT patch antenna at the frequency 10 GHz [11].

M. Dashti and **Dr. J. D. Carey (2018),** designed circular graphene patch antenna by using CST software for THz communications. They used graphene instead of metallic material (copper) to make the proposed antenna capable of transmitting and receiving large amounts of data [12].

Bengio et al **(2019),** conducted the measurements of the radiation efficiency of patch antennas made of carbon nanotube films, where the measured radiation efficiency was (94%) at the frequencies of 10 GHz, 14 GHz that matched with the equivalent copper antennas. The smallest thickness of carbon nanotube films required to match with the copper drops performance with height the frequency because of decreasing of the losses [13].

Mr. Prakasam et al **(2020),** designed and simulation of circular patch array antenna by using (FR4 epoxy) as the substrate of thickness (1.6 mm) and εr = 4.4. They used HFSS software to design and analysis 2*4 array antenna at the operation frequency of (2.4 GH_z). The return loss of this design was (-13.3235 dB) and the value of VSWR was (1.2357) [14].

Muhammad et al **(2021),** designed three types of patch array antenna (1*2, 1*4 and 2*2) and simulated it by using CST software. Their aim was to develop the gain and reduced the losses. They analyzed the gain, return loss, efficiency and radiation pattern of the designed antennas at the operation frequency 2.4 GHz. They used FR4 (lossy) as substrate placed between the patch and ground with (ε_r = 4.7) and thickness (1.6 mm) [15].

Most of the previous studies about the microstrip patch antenna focused on the use of copper in its design and manufacture on different substrates (different dielectric constant) with different thicknesses. The choice of the patch geometry depends on the nature of the application system in which it will be used. In the studies that followed, nanomaterials were used in the design and implementation of these antennas in certain ways to replace the copper [13,16].

In this search, a carbon nanotube was used to coat the fabricated copper based patch antenna on FR4 substrate with a fixed thickness of 1.6 mm and ε_r=4.3. The rectangular shape was chosen because it is commonly used and gives good results. An array of the patch elements was formed consecutively or parallel to improve the performance of the antenna and increase its gain and directivity.

1.4 Aims of the thesis

The main objectives of this thesis are

i. To design and fabricate copper-based microstrip patch antennas, which operate at radio frequencies 2.4 GHz.
ii. The proposed antennas are manufactured and tested experimentally within the operating frequency by using Nano VNA device.
iii. Design several forms of rectangular-MPA based on copper and carbon nanotube (CNT) including the single and the array, after success by designing these antennas at certain frequencies their main properties were analyzed to see the effectiveness of CNT in design and fabrication these antennas after comparing them with copper-based antennas.
iv. To coat the copper-based microstrip patch antennas with multiwalled carbon nanotube.

1.5 Summary of the thesis

Chapter One which include a general introduction from the antennas, introduction of microstrip antenna , a literature review of previous studies, the main objective of the thesis and outline of the thesis.

Chapter Two introduces introduction of microstrip patch antenna, the components of the MPA, radiation mechanism of MPA, fundamental properties of MPA, the advantage and disadvantage of MPA, the analysis methods of rectangular MPA, the array of MPA, carbon nanotube material, types of CNT , properties of CNT, features of CNT, CNT MPA and applications of MPA.

Chapter Three contains the introduction , materials, software, design of rectangular MPA and fabrication process of rectangular MPA.

Chapter Four contains the introduction, results of the designs, comparation of results for all designs, results of the fabricated antennas and discussion of the experimented results.

Chapter Five includes the most important work conclusions and recommendations for the future work.

Chapter Two

Theoretical Approach of Microstrip Patch Antenna

2.1 Introduction

The microstrip patch antenna (MPA) was first introduced in the 1950s, yet this invention waited for twenty years to be achieved after the introduction the technology of printed circuit board(PCB) in the 1970s. Since this time, the MPA is considered one of the most widely used types of antennas with wide applications due to its many advantages that we will be mentioned in this chapter later. In the 1980s, patches were used in arrays. Technology of the microstrip patch evolved and entered the systems of the commercial in the 1990s where the MPA was initially used for the communications of the mobile. Different versions of MPA were made up relying on the companies within the specifications of the required performance [3, 17].

As a result of the development of communication system engineering, this requires the development of antennas with multiple features with the survival of high performance on a wide range of frequencies. To achieve this purpose, it has been designed the MPA. The MPA includes four parts: patch, substrate, ground and feeding part as in the figure (2.1) which shows the parts of the MPA [18, 19].

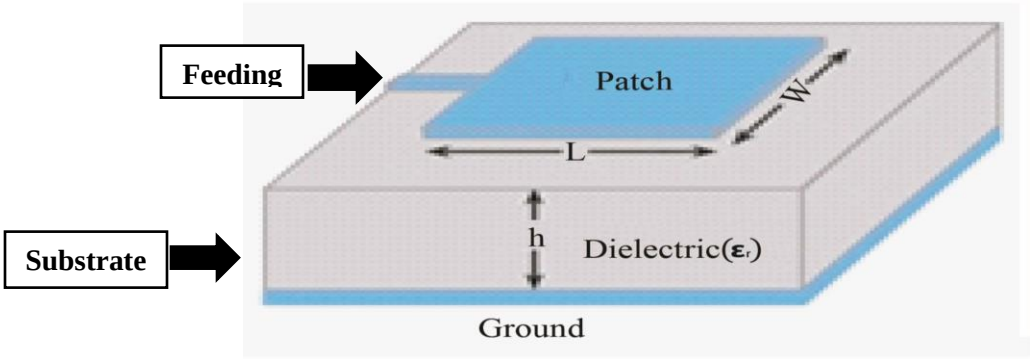

Figure (2.1) Structure of rectangular MPA

The patch made of a metallic conducting material, which is usually the copper or a nanomaterial like carbon nanotube (CNT), silver nanoparticle and more. We will

explain the CNT nanomaterial in another section of this chapter. There are many shapes of patch as shown in the figure (2.2), but circular and rectangular configurations are mostly used. Feeding part can be designed in more than one way [18, 20].

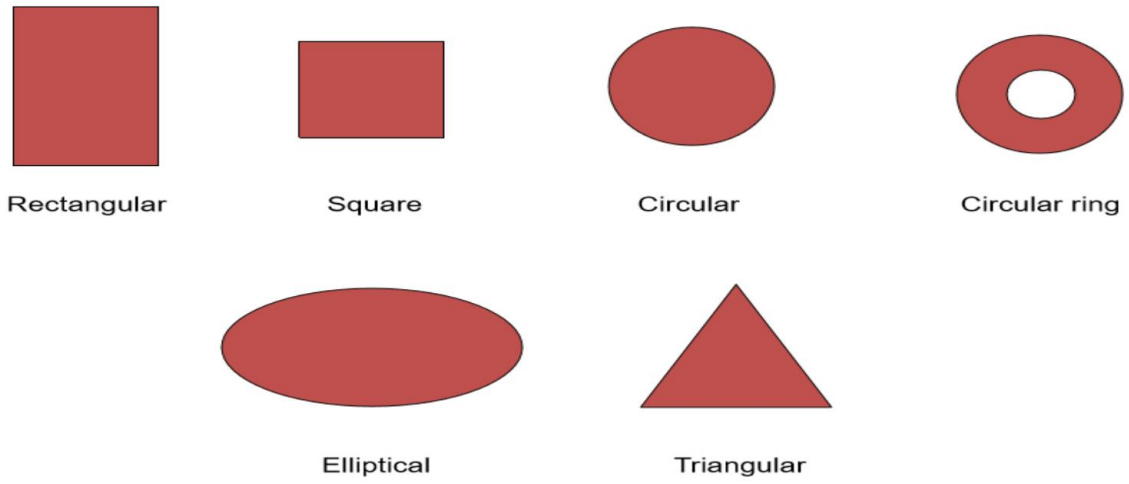

Figure (2.2) different shapes of patch

2.2 Parts of rectangular MPA

2.2.1 Patch

It is printed on the substrate, the length of the rectangular patch (L) is usually ($0.333\lambda o<L<0.5\lambda_o$), λ_o is the wavelength in free-space [21]. Width of the rectangular patch (W) controls the input impedance. The thickness of the rectangular patch (t) is very thin ($t << \lambda_{0)}$ [22].

2.2.2 Substrate

It is a dielectric material placed between the patch and ground as a dielectric material with a specific height (h) and dielectric constant (ε_r), where thickness or height (h) of the substrate is generally ($0.003\ \lambda_0 \leq h \leq 0.05\ \lambda_0$) and relative permittivity (ε_r) of the substrate is usually in the range($2.2 \leq \varepsilon_r \leq 12$) [22 , 23].

2.2.3 Ground

It is placed under the substrate and made of a conductive metal material that is usually the copper [23].

2.2.4 Feeding

Techniques of feeding are classified into several methods:

a- Microstrip line feed

There are two methods of this type (Edge feed and Inset feed) as shown in the two figures (2.3a and 2.3b). It is widely used because of its simplicity of design, analysis and ease of fabrication. In the ends of the patch, the current (I) is low and it is rised forward the center of patch. So it can reduce the input impedance (z) by feeding the patch near from its center where the input impedance inversely proportional to the current according to the law (Z=V/I) [2, 24, 25].

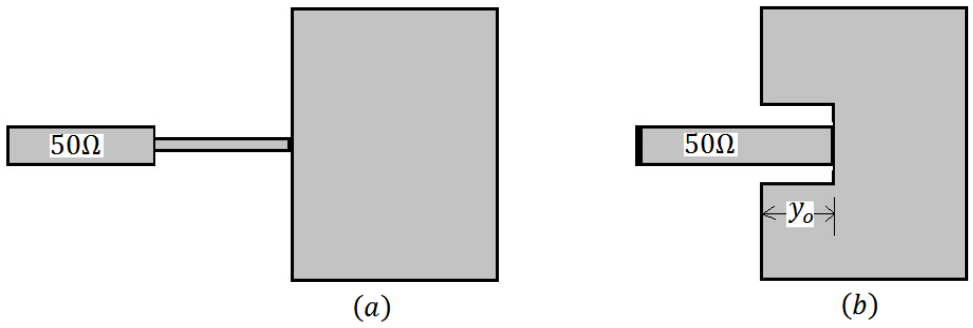

Figure (2.3) Edge feed and Inset feed of rectangular MPA

b- Coaxial Probe Feed

In this method, the outer conductor of the coaxial feed is coupled to the ground of the rectangular MPA (R- MPA), and the inner conductor is passed through the substrate and welded to the patch as shown in the figure (2.4). The major feator of this type is that the feed can be located anywhere internal the patch so as to match the probe impedance for the input impedance of the patch. This way has low false radiation. The main defect of this type is that it produces small bandwidth [24, 25].

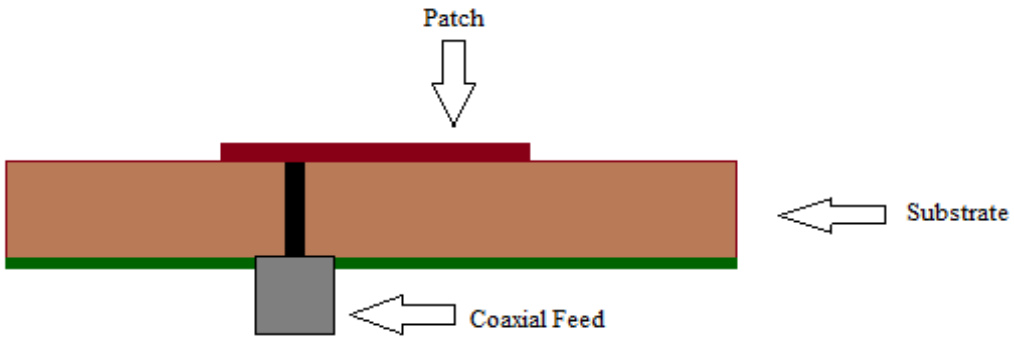

Figure (2.4) Coaxial Probe Feed of R- MPA

c- Aperture coupled feed

In this type of feeding Techniques, the patch is separated from the feed line by the ground. The patch is coupled to the line of feeding by the gap in the plane of the ground as in the figure (2.5). Here, there are two substrates, the patch is placed on the top substrate and the feed line is placed under the bottom substrate. The main disadvantage of this type is Difficulty manufacturing due to multilayers that increase the thickness of MPA .Also it produces small bandwidth [24, 25].

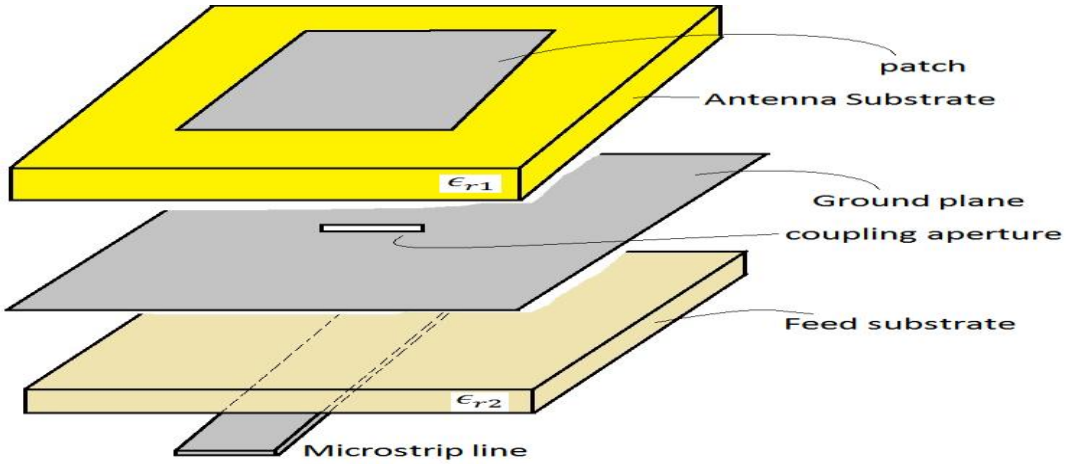

Figure (2.5) Aperture coupled feed of R- MPA

d- Proximity coupled feed

In this method, the line feed is placed between two substrates; the patch is on the upper substrate. Each substrate has its dielectric constant different from the second **(ε_{r1}, ε_{r2})** as shown in the figure (2.6). This type refers to as (an electromagnetically coupled patch antenna).The mechanism of the work between the patch and the feed line is capacitive. This type is somewhat complex in its design and analysis Because of the capacitive coupling effect between the patch and the feed line [2, 24].

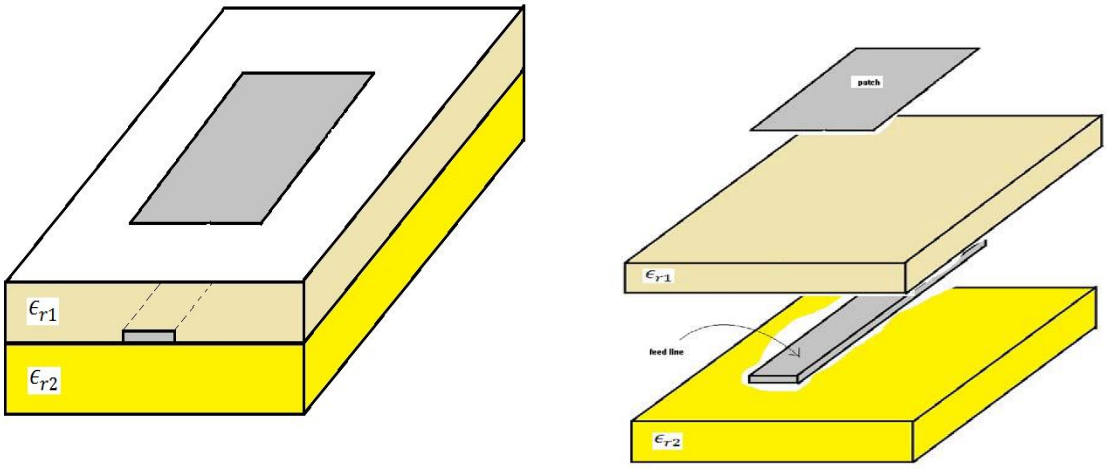

Figure (2.6) Proximity coupled feed of R- MPA

2.3 Radiation mechanism of R-MPA

In Microstrip antenna, It is the fringing fields that are responsible for the radiation. The fringing fields around the antenna can help explain why the microstrip antenna radiates. Consider the side view of a patch antenna, shown in figure (2.7). The current at the end of the patch is zero and the current is maximum at the center of the half-wave patch. Since the patch antenna can be viewed as an open circuited transmission line, the voltage reflection coefficient will be 1. When this occurs, the voltage and current are out of phase. Hence, at the end of the patch the voltage is at a maximum (say +V volts). At the start of the patch antenna (a half-wavelength away), the voltage must be at minimum (-V Volts). Hence, the fields underneath the patch will resemble, which roughly displays the fringing of the fields around the edges [18].

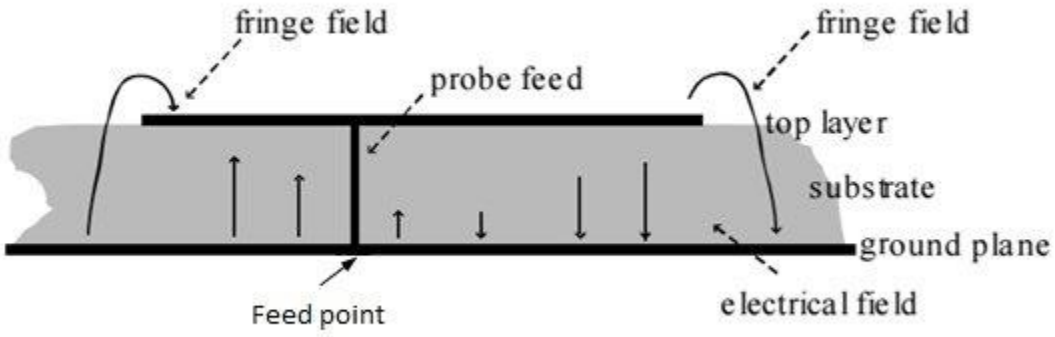

Figure (2.7) Explain how does R-MPA radiate [18]

Note that the fringing fields near the surface of the patch antenna are both in the +y direction. Hence, the fringing E-fields on the edge of the microstrip antenna add up in phase and produce the radiation of the MPA. The microstrip antenna's radiation

arises from the fringing fields, which are due to the advantageous voltage distribution; hence, the radiation arises due to the voltage and not the current. The patch antenna is therefore a "voltage radiator", as opposed to the wire antennas, which radiate because the currents add up in phase and are therefore "current radiators" [18].

2.4 Fundamental properties of MPA

2.4.1 Return loss

The return loss or the reflection coefficient is known as the ratio of the transmitted power towards the antenna to the reflected power from it. Its mathematical equation (2.2) [2].

$$\mathbf{S_{11} = 10 \log_{10} (P_{tra}/P_{ref})} \quad \mathbf{dB} \qquad (2.1)$$

$$\mathbf{RL = | S_{11} |} \qquad (2.2)$$

Where,

RL = the return loss

P_{tra} = the transmitted power to antenna

P_{ref} = the reflected power from antenna

When the value of the ratio (P_{tra}/P_{ref}) is large so the process of transmitting the power from the source to the antenna is good thus, the return power from the antenna is less. The return loss is considered a basic parameter when analyzing the antenna to know the performance of its work at the operation frequency. The value of (S_{11}) in dB must be less than (-10 dB) in order to work the antenna well within the range

of the required frequency. The return loss is the magnitude of (s_{11} parameter), which also known as reflection coefficient that symbolized by (Γ) [2].

2.4.2 Voltage standing wave ratio

It is considered as a function of the return loss, where it describes the reflected power from the antenna. It is abbreviated as VSWR. The value of VSWR is commonly a positive number and ranging between one and two in order to have antenna performance is high. If the value of VSWR is 1.0, this means that there is no return power from the antenna and in this case it is considered ideal. The Mathematical expression of VSWR in the equation (2.3) [26].

$$\mathbf{VSWR = (1 - \Gamma) / (1 + \Gamma)} \qquad (2.3)$$

2.4.3 Directivity

The rate of intensity of the radiation in a specific direction for the antenna to the average of the radiation intensity in all directions.

The total radiated power from the antenna divided by (4π) is represents the average of radiation intensity. To find the directivity of (a nonisotropic source) divided the intensity of radiation in a specific direction to the radiation intensity of an isotropic source as in the mathematical equation (2.4) [27].

$$\boldsymbol{D = U / U_0 = 4\pi\, U / P_{rad}} \qquad (2.4)$$

Where

D = the directivity (without units)

U = the radiation intensity (W/unit solid angle)

U_0 = intensity of radiation of the isotropic source (W/unit solid angle)

P_{rad} = total radiated power (W)

When the direction is not custom, it refers to intensity of the maximum radiation, then the directivity will be maximum according to the equation (2.5) [27].

$$\mathbf{D_{max} = D_0 = U_{max} / U_0 = 4\pi\ U_{max} / P_{rad}} \qquad (2.5)$$

Where,

D_{max} = D_0 = the maximum directivity (without units)

U_{max} = intensity of the maximum radiation (w/unit solid angle)

Directivity is quantity devoid of units because it is the rate of the intensity of two radiations. It is usually represented in dB_i [27].

2.4.4 Gain

The gain is the rate of intensity of the radiation in a custom direction to intensity of the radiation that can be geted when the power be radiant isotropically. Gain is Calculated by comparison intensity of the radiation when the real experiment antenna and an isotrope have the like input power. The isotrope is supposed to transmit own full input power, but part of the received power to the real antenna may be get lost in the resistance where transformed into heat. The mathematical equation (2.6) to calculate the antenna gain [28].

$$\mathbf{G = K\ D} \qquad (2.6)$$

Where,

G = gain of the antenna

K = the antenna efficiency

Efficiency of the antenna is the rate of the transmitted power from the antenna to the whole entered power. The value of antenna efficiency ranging between zero and one, where $0 \leq k \leq 1$ [28].

The gain is a unitless quantity because it is product of multiplying the efficiency by the value of the directivity (directivity is unitless).It is commonly represented in dB (decibels). To transform the gain in terms of dB, we use the formula in the equation (2.7) [28].

$$G_{dB} = 10 \log_{10} G \qquad (2.7)$$

Where, (G_{dB} = the antenna gain in decibels)

2.4.5 Bandwidth

It is known as the range of frequencies at which the antenna performance well and works properly. The BW of the broadband antennas is equal to the rate of the upper frequency to the lower frequency, While BW of the narrowband antennas is equal to the percent of the frequency difference between upper and lower frequency divided to the center frequency, as in the equations (2.8) and (2.9) [26, 27].

$$BW_{broadband} = (F_H / F_L) \qquad (2.8)$$

$$BW_{narrowband} (\%) = (F_H - F_L / F_c) * 100 \qquad (2.9)$$

Where,

F_H = the upper frequency

F_L = the lower frequency

F_c = the center frequency

2.5 Advantage and disadvantage of MPA

There are a lot of features that make use of the MPA is wide in the wireless communication, we mention some of them: low cost and it easily fabricated, light weight and small in size, it has a low profile, they can be printed directly onto a circuit board, it provides both of linear and circular polarization, it produces double and triple frequencies, ease of integration with the microwave integrated circuits, it can be formed as an array to improve the working performance and they are becoming very widespread within the mobile phone market [29, 30] .

While the disadvantage of MPA: it has low gain and efficiency, bandwidth is narrow, activity of surface waves and an external radiation comes from the feeds and junctions [29, 30].

2.6 Analysis of R-MPA

There are several methods for R-MPA analysis, but the most famous are (transmission line model and cavity model) [31].

2.6.1 Transmission line model

In this method, we suppose that the patch is (TL) or (a part of TL). It is considered the simple way to study R-MPA analysis. The R-MPA is in the form of two emitting slots that are isolated by a space (L) as shown in the figure (2.8) [31].

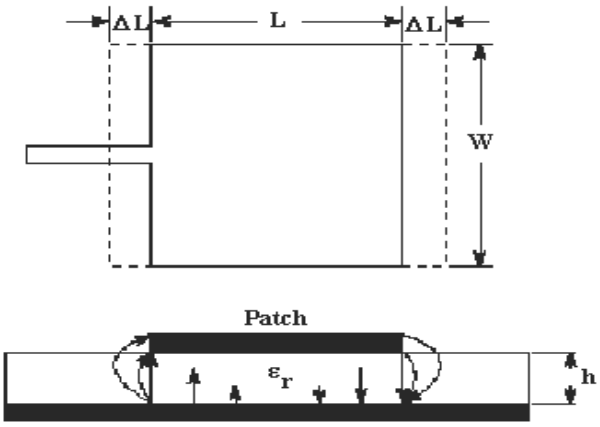

Figure (2.8) TL model

Because of the effects of fringing, the real length or effective length of the patch (L_{eff}) is equal the sum of the patch length (L) and the extra length (2ΔL), where the MPA looks appears electrically wider due to the fields of fringing [31].

Mathematical formulas of (L, L_{eff}, ΔL) and the essential parameters that we need to design the R-MPA we will mention in the equations (2.10) to (2.16) [32].

$$W = \frac{c}{2f_r\sqrt{\frac{(\varepsilon_r+1)}{2}}} \qquad (2.10)$$

Where

ε_r = dielectric constant of substrate

W =the patch width

f_r = the resonant (operating) frequency

C = speed of light in space (C= 3×10^8 m/s)

From equation (2.10), we get the width of R-MPA after substituting the values of (c, f_r , ε_r) .

$$\varepsilon_{reff} = \frac{\varepsilon_r+1}{2} + \frac{\varepsilon_r-1}{2}\left[1+12\frac{h}{W}\right]^{\frac{-1}{2}} \quad (2.11)$$

Where

ε_{reff} = effective dielectric constant

h = thickness (height) of the substrate

t = thickness (height) of patch = thickness of ground

From equation (2.11), we get the effective dielectric constant after substituting the values of (ε_r , h , w).

$$\Delta L = 0.412h\frac{\left(\varepsilon_{reff}+0.3\right)\left[\frac{W}{h}+0.264\right]}{\left(\varepsilon_{reff}-0.258\right)\left[\frac{W}{h}+0.8\right]} \quad (2.12)$$

Where

ΔL = the length extension

From equation (2.12), we get The length extension after substituting the values of (h, ε_{reff} , w, h).

$$L_{eff} = \frac{c}{2f_r\sqrt{\varepsilon_{reff}}} \quad (2.13)$$

Where

L_{eff} =effective length of patch

From equation (2.13), we get the effective length of the patch after substituting the values of (c , f_r , ε_{reff}).

$$L = L_{eff} - 2\Delta L \quad (2.14)$$

Where

L = the patch length

From equation (2.14), we get the length of the patch after substituting the values of ($L_{eff,}$ ΔL).

$$W_s = 2 \times W \quad (2.15)$$

Where

$w_{s=}$ the width of substrate = the width of ground (w_g)

From equation (2.15), we get the width of the substrate after substituting the value of (w).

$$L_{s=} 2 \times L \quad (2.16)$$

Where

L_s= length of the substrate = length of the ground (L_g)

From equation (2.16), we get the length of the substrate after substituting the value of (L).

The TL model produces a well prediction for the resonant frequency because it is taken into account the effect of the fringing fields at the ends of the patch. It is also rather accurate in predicting the MPA input impedance.It neglects the effects of the dielectric substrate and the ground plane and it does not produce insight of the radiation patterns of the MPA. Lastly, the results obtained from this model are not very accurate when we compare them with other methods, but they are well enough for R-MPA design [31].

The figure (2.9) indicates by the dimensions of R-MPA.

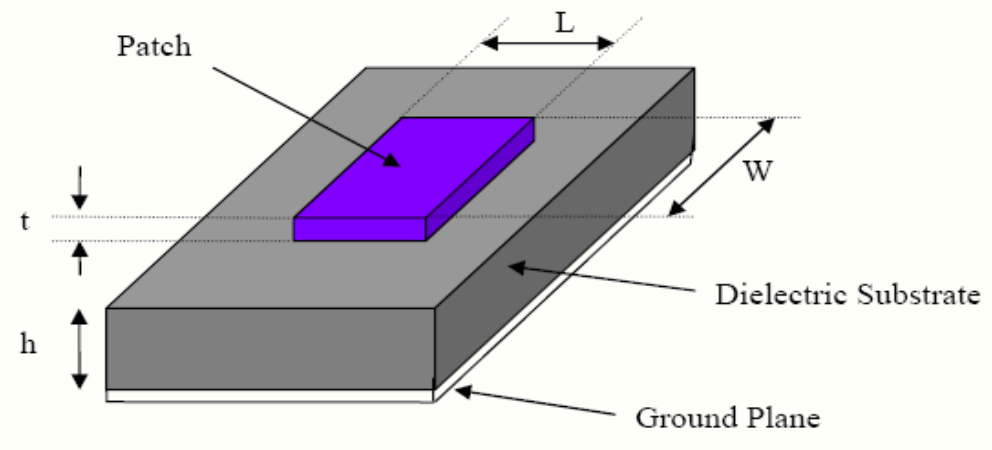

Figure (2.9) Explains visas of the R-MPA parameters [32]

To calculate the dimensions of inset feed, we used the equations (2.17) to (2.21) [33]:

$$f_i = \frac{\cos^{-1}\left(\sqrt{\frac{Z_o}{R_{in}}}\right)}{\frac{\pi}{L}} \quad (2.17)$$

Where

f_i = length of the feed inset

Z_0 = equivalent to the feed line impedance

R_{in} = the resonant input resistance

$$B = \frac{377\pi}{2Z_0\sqrt{\varepsilon_r}} \quad (2.18)$$

$$W_f = \frac{2h}{\pi}\left\{B - 1 - \ln(2B-1) + \frac{\varepsilon_r - 1}{2\varepsilon_r}\left[\ln(B-1) + 0.39 - \left(\frac{0.61}{\varepsilon_r}\right)\right]\right\} \quad (2.19)$$

$$L_f = 3.96 \times W_f \quad (2.20)$$

Where

W_f = the feed line width

L_f = the feed line length

$$G_{pf} = \frac{c \times 4.65 \times 10^{-9}}{f_r\sqrt{2\varepsilon_{reff}}} \quad (2.21)$$

Where,

G_{pf} = the gap feed line spacing

From the above equations for the inset feed, we calculate (w_f, L_f, f_i, G_{pf}).

The figure (2.10) explain the R-MPA feeding by the inset feed method and including the dimensions [33].

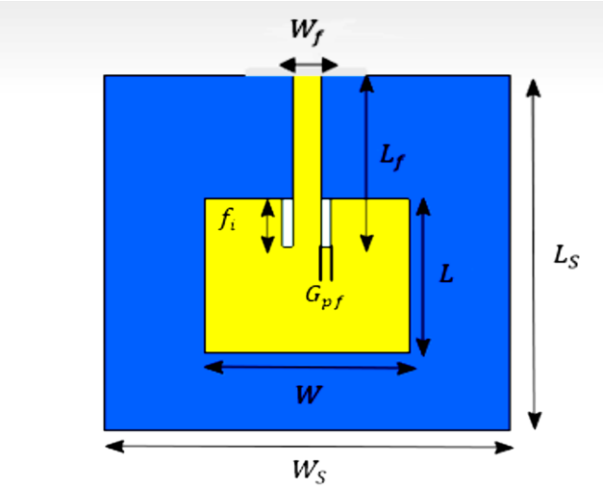

Figure (2.10) R-MPA feeding by inset feed

2.6.2 Cavity model

This method of MPA analysis is based on the assuming that the region between the patch and the ground is a resonant cavity whose ceiling and floor are electrical conductors and magnetic walls along the ends of the conductor as in the figure (2.11) [32, 34] .

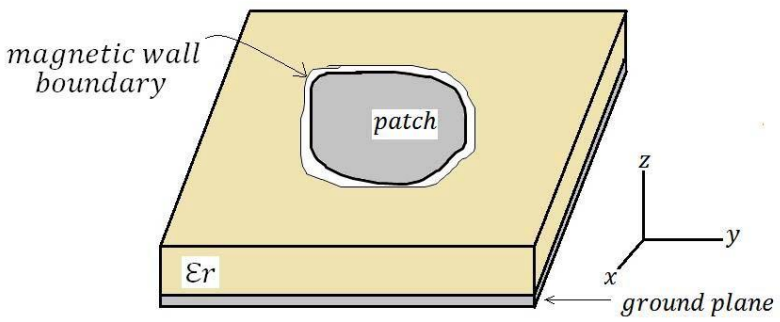

Figure (2.11) Magnetic wall model of R-MPA

If the MPA is energized by the microwave source, the charge division will establish on the top and bottom plane of the patch. Also the charges induces on the ground surface as shown in the figure (2.12) [32, 34].

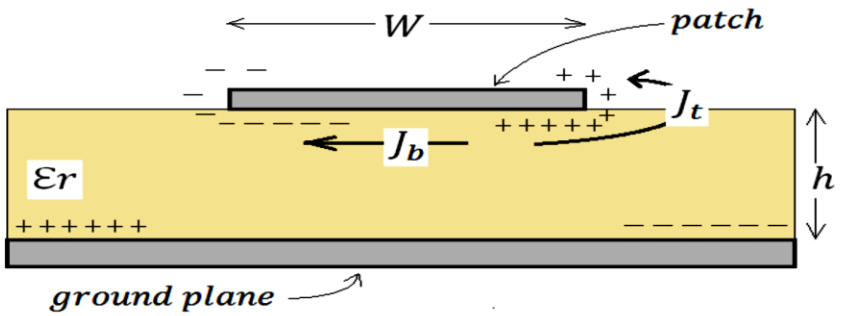

Figure (2.12) Cavity model of R-MPA

The attraction force between the different charges below the patch and on the ground surface makes concentration of the charges inner the substrate (dielectric) at the patch lower and produces the current density (J_b). The repulsion force between the similar charges upper and lower the patch produces the current density (J_t) [32, 34].

2.7 Array of MPA

The MPA is used in arrays in addition to the singular elements, where connect a group of MPA elements in a specific way to form an array of antennas. The purpose is to improve the MPA performance and to develop its basic properties such as gain,

directivity, radiation pattern and other functions that are difficult to obtain when using a single element of the MPA. Signal to noise ratio (SNR) in the array of MPA is more than there in the single MPA. Because of the proximity between the patches, there is an interaction between the array elements. This causes coupling between the patch elements, as each element of the patches [32].

For the design of the MPA array, there are basic points to form the general pattern of the antenna [32]:

1-Geometry configuration of the total matrix (linear, circular, planar).
2-The spacing between the elements of array antenna.
3- The amplitude and Phase of excitation for each element.
4-The radiation pattern for each element.

The far field of a uniform array is equal to the single element field multiplying by the array factor, as follows [32]:

$$\mathbf{E_{total} = [\ E_{single\ element}] \times [array\ factor]} \qquad (2.22)$$

$$\mathbf{Array\ Factor = \Sigma^{N}_{n=1} (\ e^{j(n-1)}\ \Phi} \qquad (2.23)$$

$$\mathbf{\Phi = kd\ cos\theta + \beta} \qquad (2.24)$$

Where , N = number of array elements
θ = scan angle

There are many types of networks of the feeding for MPA array that depends on the arrangement the elements of the patches in the array, this types are series-feed

network, corporate feed network or common between them, as in the figure (2.13) [32, 35] .

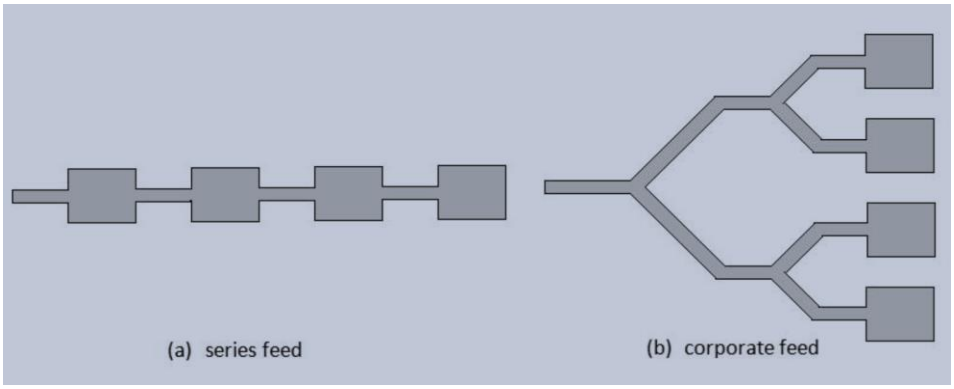

Figure (2.13) series feed, corporate feed of MPA

2.8 Carbon nanotube nanomaterial

Nanomaterials science is an emerging and rapidly developing research field. The material differs at the nanoscale from its natural state in terms of the basic properties of the material, where it is more effective such as electrical, mechanical and magnetic properties and thus plays an active role in the installation and development of modern electronics [36].

One of the nanomaterials is carbon nanotube (CNT), which was discovered by Sumio Iijima in 1991 [39]. CNT is a honeycomb cross section rolled into an empty barrel with nm measurement and μm length [37, 38]. The expansion of material theory and the betterment of fabrication technology, nano-phase materials have gained great interest in different fields due to their uncommon properties. They can be applied in many specialties such as electrics, biology, chemistry, and physics. Over recent years, vast progress has been made in the discovery and innovation of nano phase materials used in the electromagnetic field, leading to the growing interest in the research of the properties of varied nano-structured composites [39].

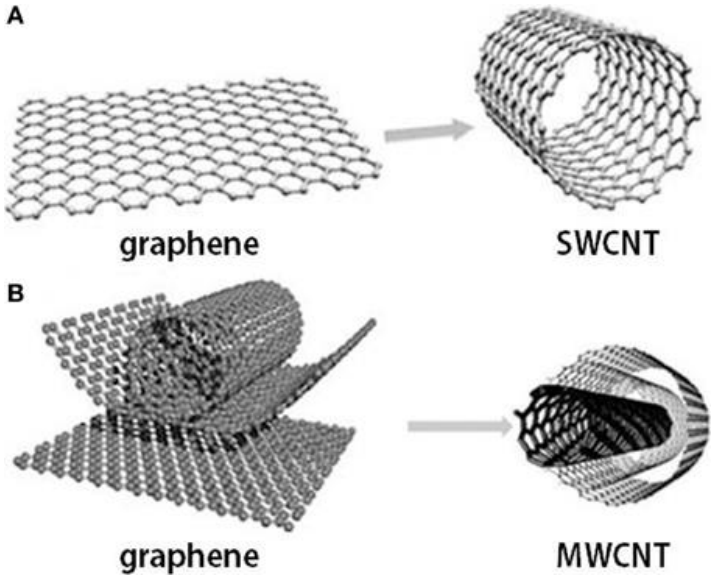

Figure (2.14) geometric shape of SWCNT and MWCNT [36]

CNT is cylinders consisting of several layers of graphene. Figure (2.15) represents image of CNT under scanning electron microscopy (SEM) [40].

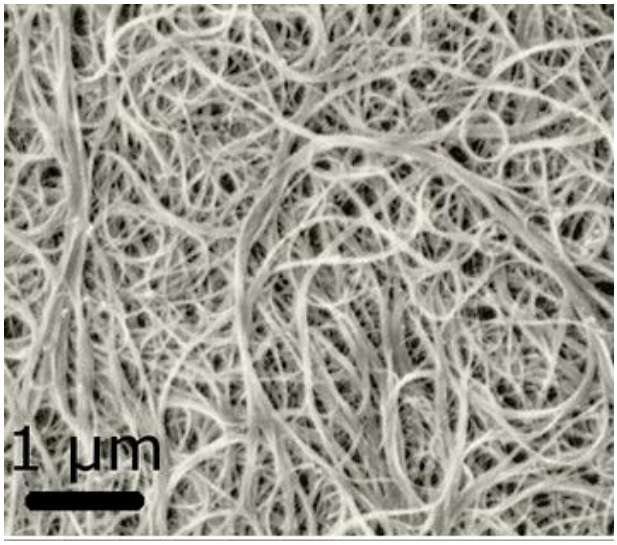

Figure (2.15) SEM image of CNT [40]

2.8.1 Types of CNT

CNT is divided into two types:

1) Single Walled Carbon Nanotube (SWCNT)

SWCNT consists of a singular cylinder-shaped carbon coat with a diameter in the domain of 0.4-2 nm, relying on the temperature at which they have been synthesized. It was found that the top the growth temperature greater is the diameter of CNT. The construction of SWCNT likely zigzag, chiral, or helical provisions. The SWCNT has a high surface space about 1300 m^2/g. SWCNT is recognized to be more efficient than MWCNT. This is due to the cause that SWCNT has ultra-high surface space [41].

2) Multi-Walled Carbon Nanotube (MWCNT)

MWCNT consists of sundry coaxial tubes, all made of a single graphene sheet framing a deep core. The external diameter of MWCNT ranges from 2-100 nm, however the internal diameter is in the range of 1-3 nm, and their tallness is one to several micrometers. The sp^2 crossbreeding in MWCNT, an unlimited electron cloud over the hedge is created which is accountable for the interactions between together cylindrical coats in MWCNT causing in a lower elastic and more structural weaknesses. MWCNT constructions can be cleave into two types depending on their arrangements of graphene coats one owns a parchment as construction which contains of a graphen piece rolled up about it and the other is recognized as the Russian dolly model where coats of graphene pieces are harmonious inside a concentric construction decoration of MWCNT contains of putting nano-particles

on the MWCNT walls, bonded by physical contact with possible applications in magnetic data storage, biosensors, and electronic instruments [41].

2.8.2 Properties of CNT

Properties of CNTs are quite different than the material we generally use. These properties made CNTs such important material for using in nano technology and also in high frequency region. Some properties are discussed below in general:

1- Strength

Carbon nanotube have a strength of tensile higher than steel and Kevlar. Their strength derives from the sp^2 chains between the atoms of the singular carbon. This chain is stronger than the sp^3 chain found in diamond. Under great force, singular nanotubes can link jointly, exchange sp^2 links for sp^3 links. This provides the portability of creating tall nanotube chains. In addition to the strength of the CNT, it is also flexible. It is possible by pressing on the side of a nanotube and give rise it to droop without destructive to the nanotube, and it will come back to its authentic form once the strength is extracted [42].

The flexibility of nanotube does have a border, and under so powerful powers, it is probable to constantly disfigure to style of a nanotube. The strength of nanotube can be fallen by disorder in the nanotube construction. Failings take place from atomic gaps or a misplacement of the links of carbon. Failings in the construction can reason a tiny part of nanotube to be weakened, which reasons strength of the tensile of the whole nanotube to decay. The force of the tensile of a nanotube depends on the force of the frailest part in tube like to the method the force of a chain relies on the frailest join in the string [42].

2- Electrical properties

The construction of a CNT decides how the nanotube conductive is. Once the atoms construction in a CNT decreases the collisions among conduction electrons and atoms, a CNT is ultra conductive. The powerful links between carbon atoms too let CNT to resist great electrical currents than copper. The electron transfer occurs only over the axis of the tub. The SWNTs are able to route electric signals at velocities up to 10 GHz when used as communicates on semi-conducting devices. Nanotubs too have a fixed resistively [42, 43].

3- Thermal Properties

As rolled graphene constructions, CNTs are of big importance and benefit not only for its electronical and mechanical characteristics, as well as for their thermal characteristics. Although their volume is so tiny, the quantum effects are important and the little-temperature specific heat and thermal conductivity display direct indication of the 1-D quantization of the phonon band construction in CNTs. The combination of perfect and functionalized nanotubs to various materials can twice the thermal conductivity for a charging of only 1%, presenting that nanotube combined materials might be beneficial for thermal supervision applications in the industries. The thermal conductivity was measured of singular MWNT and it is to be 3,000 W/K at the temperature of the room. While it was for SWNTs 200 W/m K. There are many features, which effect to the thermal characteristics as the number of phonon-vigorous styles, the length of the permitted track for the phonons, and limits surface scattering. These characteristics too depend on the arrangement atomic, the diameter and length of the tubs, the number of essential failings and the morphology, in addition to the attendance of contaminations in the CNT [44, 45, 46, 47, 48, 49].

2.8.3 Features of CNT

Highly flexible nature and have the potency of delivery inside cells. It is very light in weight and does not break durining handling. It has an available terminus on both ends, makes the inside area attainable and posterior combination of types inside nanotubes is especially simple. CNTs are capable to come in cells by automatic mechanism because of its tubeform and nanoneedle form. Its own a specific inner and outer area, which can be differentially modified for chemical bio-chemical functionalization [41].

2.8.4 CNT MPA

It is known that the antennas are manufactured using metals that are characterized by their low resistance and therefore conduct and radiate good electromagnetic waves, and one of these metals is the usual copper in the manufacture of the MPA.

Recent studies in recent years have found alternatives to these metals, which are nanomaterials, which are characterized by their high electrical conductivity, lightweight, and strong mechanical properties, in addition to their tolerance of high temperatures and great resistance to various conditions of nature. Therefore, these materials entered the field of wireless applications and played an important role because of the features they provide for this system, which metals lack [13].

Examples of nanomaterials used as a MPA are carbon nanotube, silver nanoparticle, graphene, etc. What matters to us is the CNT that we will use in our research to design the MPA. CNT is used to replace copper in the fabrication of MPA. It uses in many applications such as communications, military, sports, medical and others. These require certain characteristics that must be available in the antenna

used, such as antennas that can be worn in the hand, back, helmet, or the like, which require flexibility in the used antenna [50] .

The density of CNT is less than that of copper (the density of CNT is equal to about 1.4 g/cm^3, while the density of copper is equal to about 8.96g/cm^3. The thermal conductivity of CNT is more than ten times of copper [51, 52].

CNT is characterized by additional inductive influence as compared with the conventional conductors as copper wires of the same volume. Consequently, CNT has high characteristic impedance and slow wave propagation in comparison with conventional conductors. Due to these characteristics, CNT can be used as antenna [53].

2.9 Applications of MPA

Antennas are famous for their good performance and strong industry, so their use has entered into various fields such as medical applications, satellites and military systems (missiles and aircraft). Due to its low cost, it has flourished in the commercial aspects. Some of examples of MPA applications are [54]:

a-Mobile and satellite communication application

Mobile communication requires small, low-cost, low profile antennas. MPA meets all requirements and various types of microstrip antennas have been designed for use in mobile communication systems. In case of satellite communication, circularly polarized radiation patterns are required and can be realized using either square or circular patch with one or two feed points [54].

b- Global positioning system application

In this application, the MPA is circularly polarized for high-accuracy positioning [54].

c-Radio frequency Identification (RFID)

RFID uses in different areas like mobile communication, logistics, manufacturing, transportation and health care. RFID system generally uses frequencies between 30 Hz and 5.8 GHz depending on its applications [55].

d-Radar application.

Radar can be used for detecting moving targets such as people and vehicles. It demands a low profile, light weight antenna subsystem, the microstrip antennas are an ideal choice. The fabrication technology based on photolithography enables the bulk production of microstrip antenna with repeatable performance at a lower cost in a lesser time frame as compared to the conventional antennas [56].

e-Rectenna application

Rectenna is a rectifying antenna, a special type of antenna that is used to directly convert microwave energy into DC power. Rectenna is a combination of four subsystems i.e. Antenna, ore rectification filter, rectifier, post rectification filter. in rectenna application, it is necessary to design antennas with very high directive characteristics to meet the demands of long-distance links. Since the aim is to use the rectenna to transfer DC power through wireless links for a long distance, this can only be accomplished by increasing the electrical size of the antenna [54].

f- Tele-medicine application

In telemedicine application antenna is operating at 2.45 GHz. Wearable microstrip antenna is suitable for Wireless Body Area Network (WBAN). The proposed antenna achieved a higher gain and front to back ratio compared to the other antennas, in addition to the semi directional radiation pattern, which is preferred over the omni-directional pattern to overcome unnecessary radiation to the user's body and satisfies the requirement for on-body and off-body applications [57].

g-Medicinal applications

It is found that in the treatment of malignant tumors the microwave energy is said to be the most effective way of inducing hyperthermia. The design of the particular radiator, which is to be used for this purpose, should possess lightweight, easy in handling and to be rugged. Only the patch radiator fulfils these requirements [58].

Chapter Three

Design and Fabrication of R-MPA

3.1 Introduction

In this chapter, the rectangular microstrip patch antenna (R-MPA) (single and array) was designed. First, copper was used as the radiating patch and the substrate was FR4 and also used the ground plane of copper. We have designed single R-MPA and array R-MPA, in the array four and two elements of patches were used by forming it with two ways differed in networks of the feeding (4*1 array and 1*4 array). Then, CNT used as the radiating patch with the same materials that used in the first case. Also, has worked same the designs that is done in the first case. The feeding line technology that have used is the inset feed. CST software version 18.0 used to design and simulate our designs. The operation frequency was 2.4 GHz.

On the practical side, the R-MPA was made single and array (1*2). First, we used copper to fabricate the antenna, and then we used CNT to fabricate it also. Has been used two layers printed circuit board (PCB) (top side and bottom side made of copper And the isolation layer between them is FR4) .Thickness of copper is 0.035 mm and of FR4 is 1.6 mm .We used the computer numerical control (CNC) machine to draw and dig the PCB to configure the R-MPA according to the specified dimensions. The fabricated antennas were connected with the N-type connector (SMA) for testing the antennas by Nano vector network analyzer (VNA) device, where it measured the return loss and VSWR, ..etc at 2.4 GHz.

3.2 Materials

To design the R-MPA must be choose the materials that the antenna is made of. Here, our aim is designed the R-MPA by using copper as (the patch and feed line) once, then CNT once again. There are many types of the substrate, but the FR4 was chosen as the dielectric substrate. The surface of the ground of the antenna should be conductor as the copper. Also, the inset feed was used as feed line .

3.3 Software

There are several programs for designing and simulating antennas, including: *HFSS software* (high frequency structural simulator), IE3D (Zeland software), *CST* MWS software (computer simulation technology Microwave Studio).

In our search, CST software was preferred because it provides quick and accurate analysis of high-frequency antenna designs, as it is a specialized tool for three-dimension (3D) simulation of electromagnetic waves. It also performs well, which makes it the right choice for us in research.

3.4 Design of R-MPA

The TL model is used to design the mathematical equations that it is used to calculate the essential parameters for designing the R-MPA.

Before starting the application of design of R-MPA, we must determine the operating frequency (f_r), the dielectric constant (ε_r), and the thickness of the substrate (h). Then, we use the equations of TL model from equation (2.10) to equation (2.21) to determine the dimensions of the R-MPA.

In all the designs, we used the essential parameters mentioned in the table (3.1).

Table (3.1) The essential parameters of all proposed designs

parameter	value
f_r	2.4 GH_z
h	1.6 mm
ε_r	4.3

Substituting these parameters in the equations of TL model, we get:

W = 38.39 mm w_s = 76.78 mm

L = 29.77 mm L_s = 59.54 mm

The dimensions that obtained from the mathematical calculations by means of equations, when it was used in the program (CST software), did not get very good results for the R-MPA, so is increased or decreased these dimensions by a very small amount until reached the best results for the designed antennas, and this is very normal due to the error ratio between the equations and the program. So the optimized values of the R-MPA dimensions were used in our proposed designs.

The following materials and its values are constant in use in all of our proposed designs:

The substrate is FR4 (εr = 4.3, h = 1.6 mm),

The ground is copper (t = 0.035 mm),

Thickness of copper = thickness of CNT = 0.035 mm (t).

Input impedance = 50 Ω.

The important characteristics of CNT that added in CST software are:

Electric conductivity = 185000 s/m [59]

Thermal conductivity = 3500 W/K/m [59]

Density = 1600 kg/m^3 [59]

3.4.1 Design by using copper

In this section, we have been designed the R-MPA by using copper as the radiating patch, we made three designs by using (CST software) as follows:

a) Single element of R-MPA

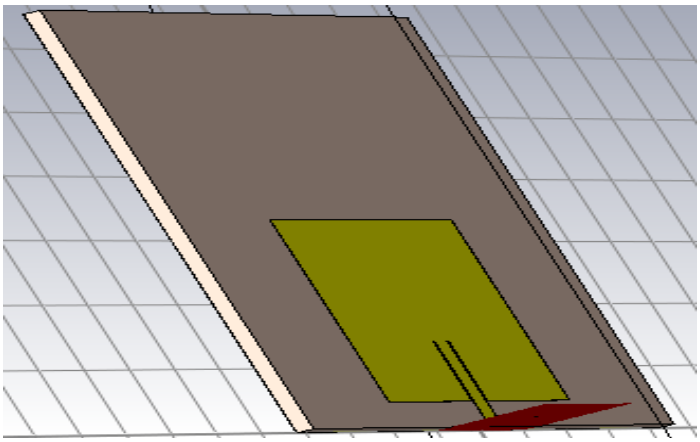

Figure (3.1) Single element R-MPA of copper (3 D)

a- Front View b- Back View

Figure (3.2) Single element R-MPA of copper (2 D)

Here, we used single element of the patch to form R-MPA as shown in the figure (3.2). The table (3.2) contains the dimensions of this design.

Table (3.2) Dimensions of single copper R-MPA

parameter	w	L	W_s=W_g	L_s=L_g	W_f	L_f	f_i	G_{pf}	h	t
value(mm)	42	32.75	84	65.5	3	13.5	9.5	0.25	1.6	0.035

b) 1×2 array elements of R-MPA

In this design, the spacing between the elements of the antenna is λ/2. Connecting the array elements is parallel through the antenna feed lines as in figure (3.3).

$\lambda = c / f = 3 \times 10^8 / 2.4 \times 10^9 = 0.125$ m = 125 mm

λ/2 = 125/2 = 62.5 mm (the distance between elements of the patches in the array R-MPA)

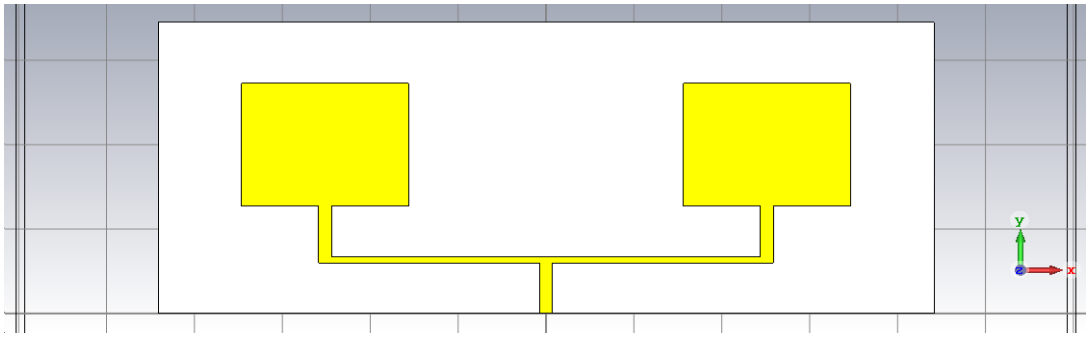

Fig (3.3) 1×2 array R-MPA of copper

Table (3.3) contains the dimensions of this design.

Table (3.3) Dimensions of 1×2 array copper R-MPA

parameter	w	L	W_s=W_g	L_s=L_g	W_f 50Ω	L_f	W_f 70Ω	h	t
value(mm)	38	29	176.5	69	3	12	1.5	1.6	0.035

c) 4×1 array R-MPA

In this design, we used a series feed to form an array of the patches consisting of four elements as shown in the figure (3.4).

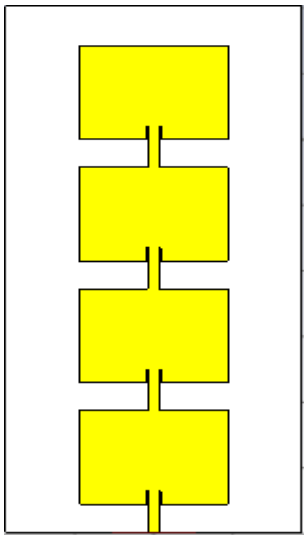

Figure (3.4) 4×1 array elements R-MPA of copper

The table (3.4) contains the dimensions of this design which was used in CST.

Table (3.4) Dimensions of 4×1 array copper R-MPA

parameter	W	L	W_s=W_g	L_s=L_g	W_f	L_f	f_i	G_{pf}	h	t
value(mm)	37.5	28.5	75	160	3	12.5	4	0.25	1.6	0.035

d) 1×4 array R-MPA

In this design the spacing between the elements of the antenna is λ/2, where we used corporate feed with arrangement the suitable impedance matched network such as in the figure (3.5).

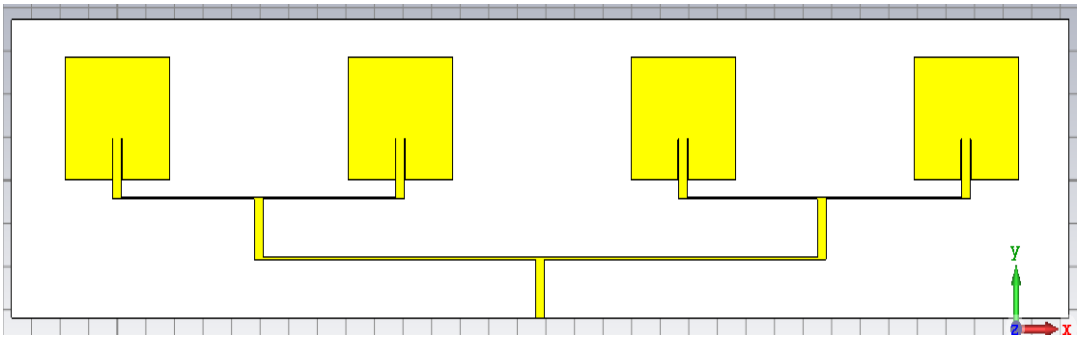

Figure (3.5) 1×4 array elements R-MPA of copper

The input impedance to each patch was 50Ω, while the impedance between the feeding lines of the elements was 70Ω to impedance matching, but the last feed line which was connected the port must be 50Ω.

Where W_f =3 mm of 50Ω and W_f = 0.4 mm of 70Ω .

The table (3.5) contains the dimensions of this design after optimization.

Table (3.5) Dimensions of 1×4 array copper R-MPA

parameter	W	L	W_s= W_g	L_s= L_g	W_f 50Ω	W_f 70Ω	L_f	f_i	G_{pf}	h	t
value(mm)	36.5	28.5	370	69	3	0.4	13.5	9.5	0.25	1.6	0.035

3.4.2 Design by using CNT

In this design, we used CNT material instead of copper material and as the radiating patch with the same materials used in the previous designs. We designed three of R-MPA as follows:

A) Single R-MPA

In this design, we used single element of the CNT patch to form R-MPA as the shown in the figure (3.6).

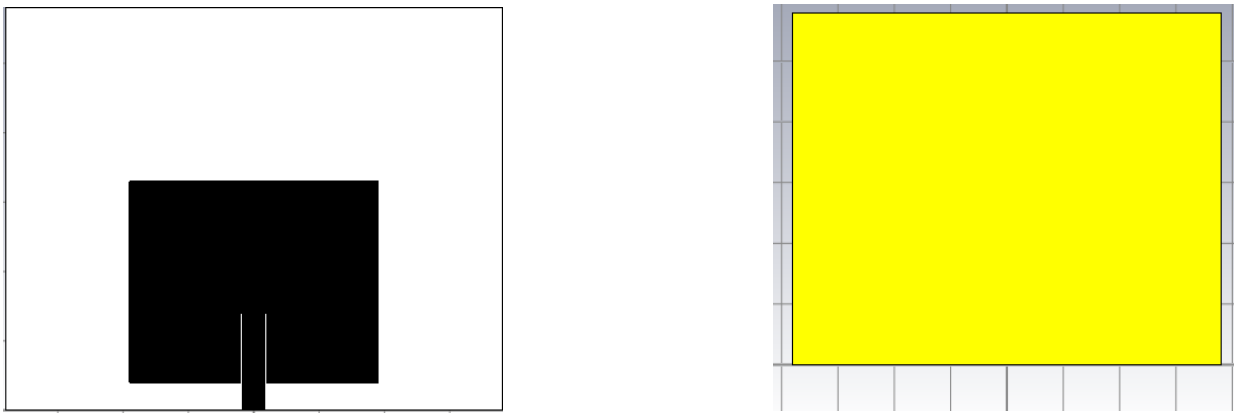

a-Front View b- Back View

Figure (3.6) Single element R-MPA of CNT (2 D)

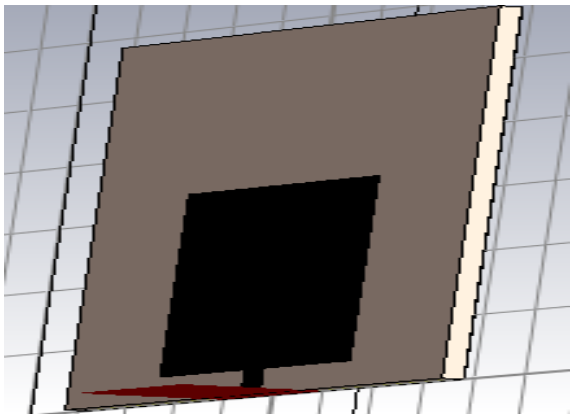

Figure (3.7) Single element R-MPA of CNT (3D)

The following table (3.6) contains the optimized dimensions of this design.

Table (3.6) Dimensions of single CNT R-MPA

parameter	w	L	W_s=W_g	L_s=L_g	W_f	L_f	f_i	G_{pf}	h	t
value(mm)	38	29	76	58	3.5	14	10	0.25	1.6	0.035

B) 4×1 array R-MPA

In this design, we used a series feed to form an array of the CNT patches consisting of four elements Where the elements are connected by one feed line as shown in the figure (3.8).

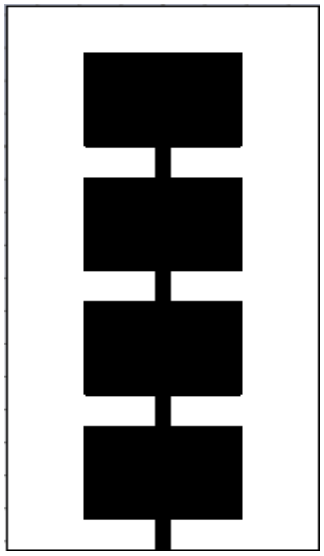

Figure (3.8) 4×1 array elements R-MPA of CNT

The table (3.7) contains the optimized dimensions of this design which was used in CST software.

Table (3.7) Dimensions of 4×1 array CNT R-MPA

parameter	W	L	W_s=W_g	L_s=L_g	W_f	L_f	f_i	G_{pf}	h	t
value(mm)	37.25	28.25	74.5	165.13	3	12.5	3	0.25	1.6	0.035

C) 1×4 array R-MPA

It is the same design of (1×4 array R-MPA of copper), Except that here we exchange copper with the CNT as the radiating patch and feed line and as in the figure (3.9).

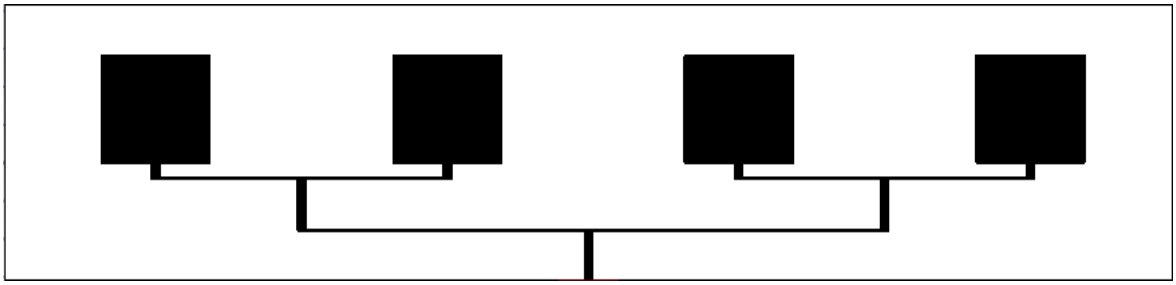

Figure (3.9) 1×4 array elements R-MPA of CNT

The table (3.8) contains the optimized dimensions of this design inside CST program.

Table (3.8) Dimensions of 1×4 array CNT R-MPA

parameter	W	L	W_s= W_g	L_s= L_g	W_f 50Ω	W_f 70Ω	L_f	f_i	G_{pf}	h	t
value(mm)	37	28.25	365	70	3	0.4	13.25	10	0.25	1.6	0.035

3.5 Fabrication of R-MPA

From the CST software, we took the dimensions (width and length) of the R-MPA to be manufactured, and they were drawn using the Altium designer winter 09 program then they were exported in the form of Gerber. We transformed Gerber formula to G-code formula by using CopperCAM program that the program of the CNC machine receive it to draw the designs. Here, we used edge feed to feeding the patch antenna.

A) Fabrication of R-MPA (by using metal only)

The following steps explain industry of R-MPA by using copper:

1) PCB double side

It consists of two layers of copper between them FR4 material.

The dimensions of it is (15 * 20) cm, thickness of copper= 0.035 mm, thickness of FR4 = 1.6 mm.

Figure (3.10) double side PCB

2) CNC machine

The file of G-code formula is opened in the program of CNC machine for cutting and holding the PCB board according to the shape to be executed.

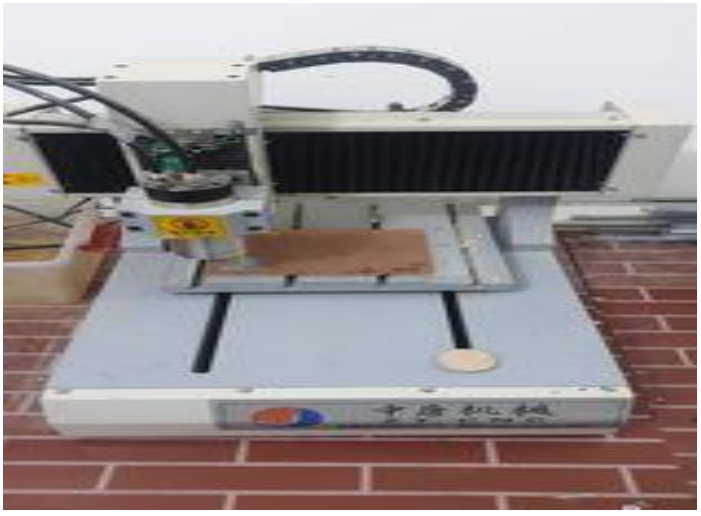

Figure (3.11) photographic image of CNC machine (ZT CNC)

3) N-type connector (SMA)

After completing the fabrication of the antenna, the antenna is soldered from the fed side with SMA connector through which Check the fabricated R-MPA.

SMA has a 50 Ω impedance.

Figure (3.12) SMA connector

4) Testing by Nano VNA instrument

Nano VNA is the device that measured an antenna characteristics such as the frequency , return loss , VSWR ,etc. As shown in figure (3.13)

Figure (3.13) NANO VNA device

Nano VNA instrument is connected to the fabricated R-MPA via SMA connector to measure antenna parameters such as the operating frequency, s-parameter, VSWR..etc. Where the frequency is determined within a certain range, work through it the antenna. The Nano VNA device used in our thesis has the ability to measure frequencies range from 50 KH_z to 3 GHz.

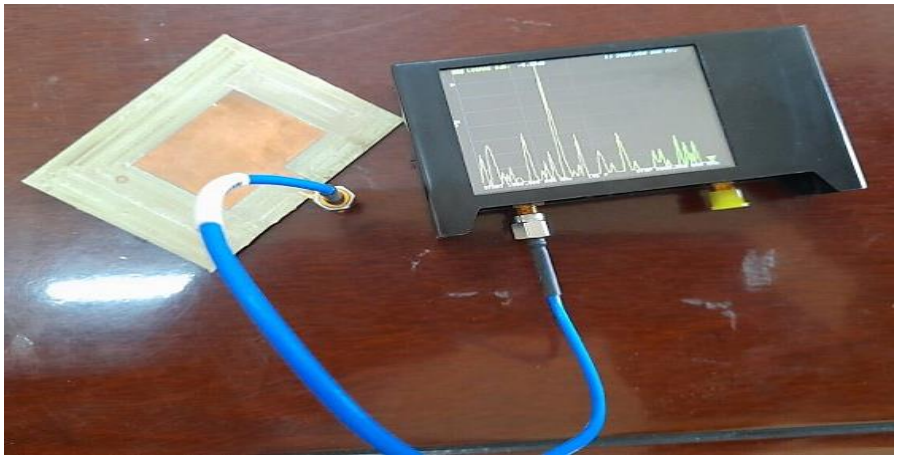

Figure (3.14) Test of the R-MPA

B) Fabrication of CNT R- MPA

Here we follow the same steps that were mentioned in the section (A) to make R-MPA. After fabrication of the antenna, ink of MWCNT was added on the surface of R-MPA, put it on the hot plate, and adjust the temperature at 120 ^{0}C and waiting for 10 minutes to dry the nanomaterial on the surface of the metal, then measuring the antenna parameters by using Nano VNA device.

Figure (3.15) explains how to coat the MPA substrate area with CNT ink. A tape was used to avoid the other part of the substrate from coating.

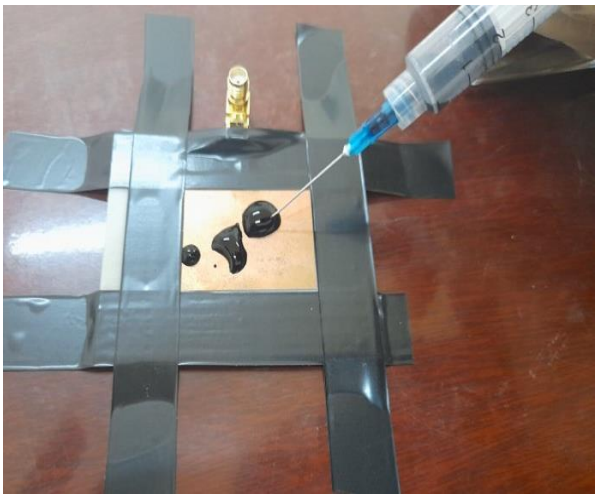

Figure (3.15) Coating of MPA with CNT ink

The nanomaterial was uniformly distributed over the metal surface as shown in figure (3.16).

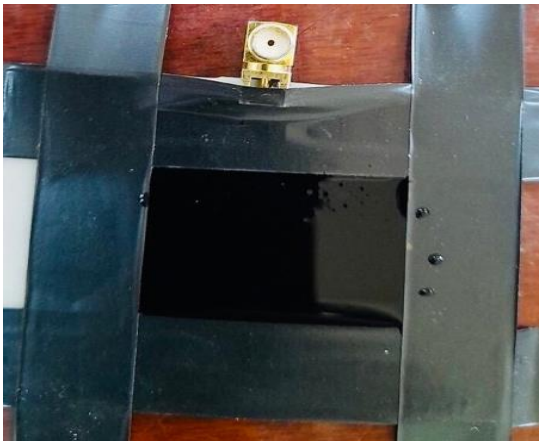

Figure (3.16) Uniformly coating of CNT ink on the copper surface

After the ink of CNT is spread regularly on the surface of the metal, the antenna is placed on the hot plate device to dry the CNT ink and to make it as solid layer on the copper layer. Figure (3.17) shows the hot plate device setting on 120 ^{O}C for 10 minutes.

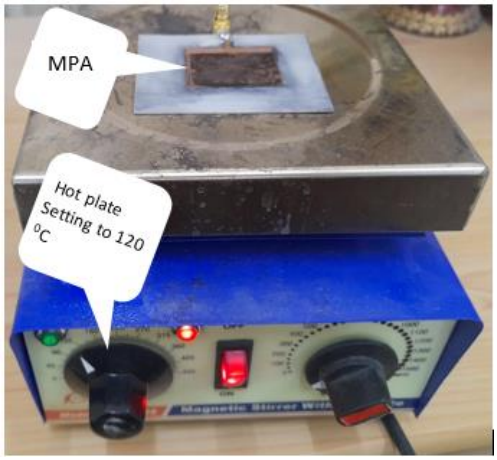

Figure (3.17) CNT R-MPA on the hot plate device

After finishing the drying process of the CNT ink, we turned-off the hot plate device and took the antenna for testing by Nano VNA. The measuring the MPA parameters were implemented as shown in figure (3.18).

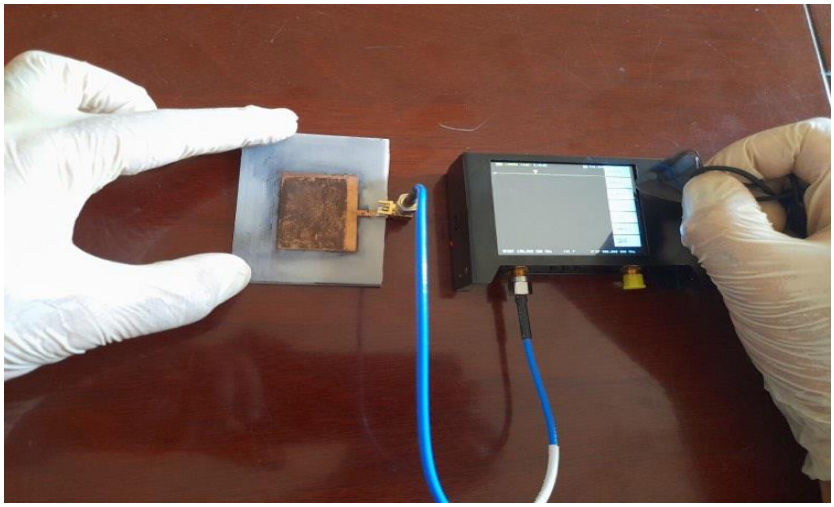

Figure (3.18) Test of the CNT R-MPA

The figure (3.19) briefly explains flow chart about the fabrication process of the R-MPA by using copper and CNT.

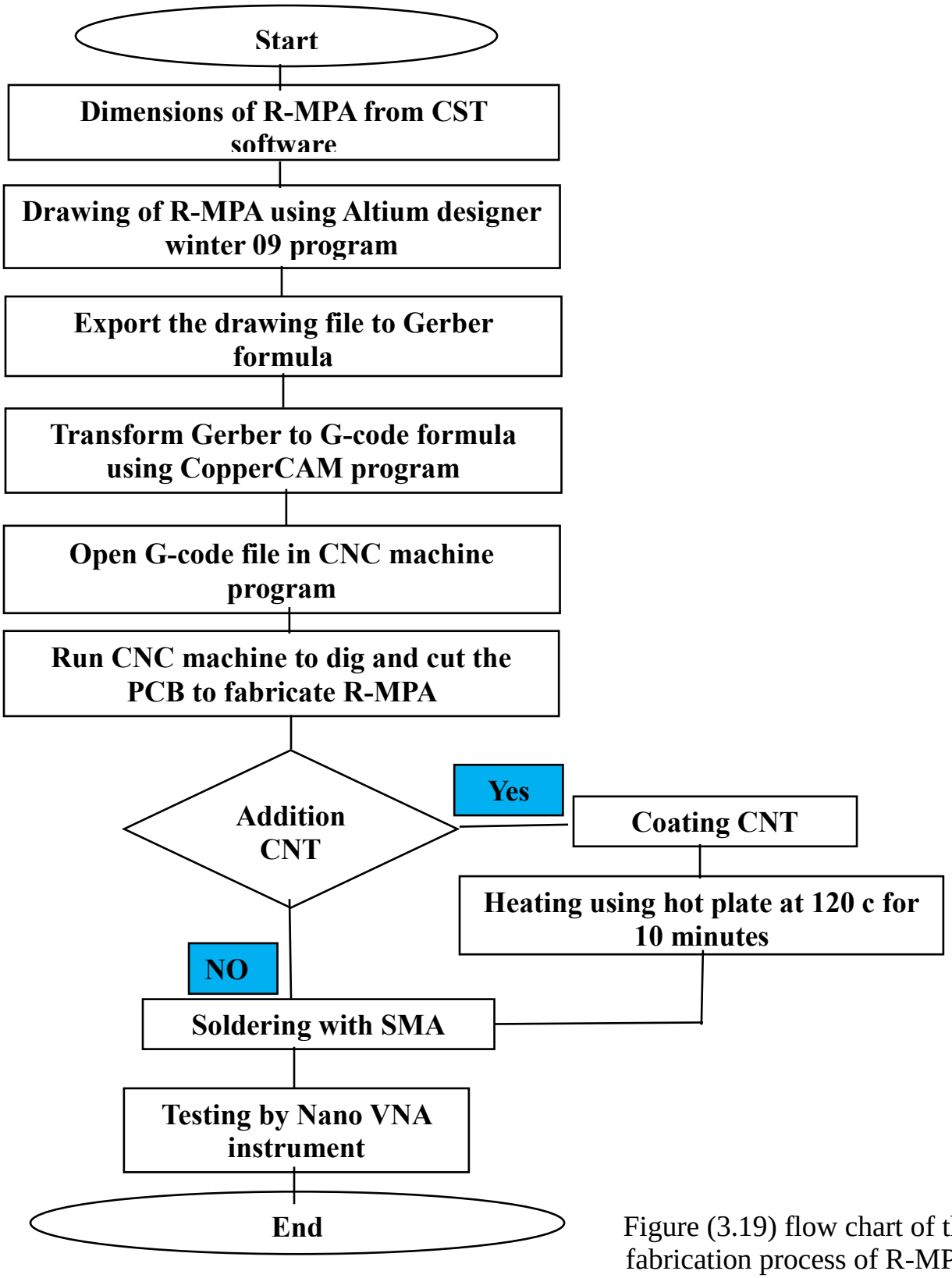

Figure (3.19) flow chart of the fabrication process of R-MPA

3.5.1 The Manufactured designs

Four designs were made (single and array), two of them without the nano-material, only copper, and two by adding the nano-material (CNT) over the copper and as in the following:

3.5.1.1 Single R-MPA

The dimensions of R-MPA are as follows:

Dimensions of patch : width * length = (37.5 * 28.5) mm

Dimensions of feed line : width * length = (3 * 12) mm

Dimensions of substrate : width * length = (75 * 57) mm

A) Copper only

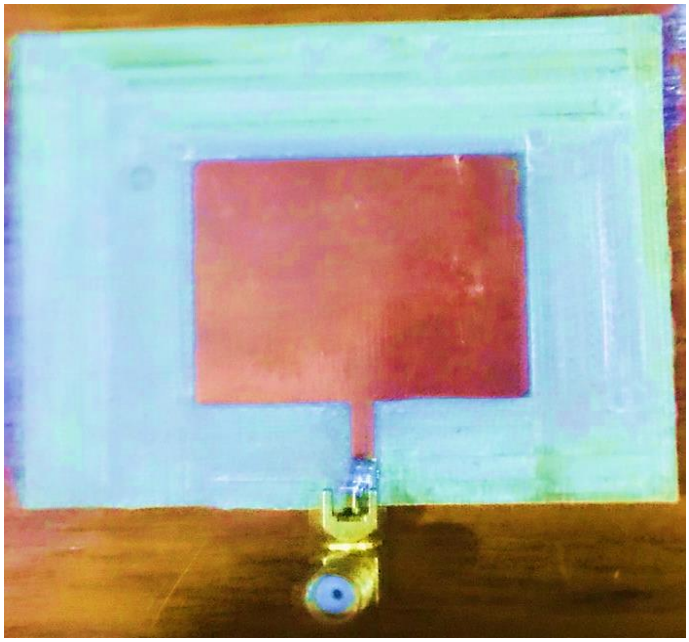

Figure (3.20) The fabricated R-MPA (single)

B) CNT with copper

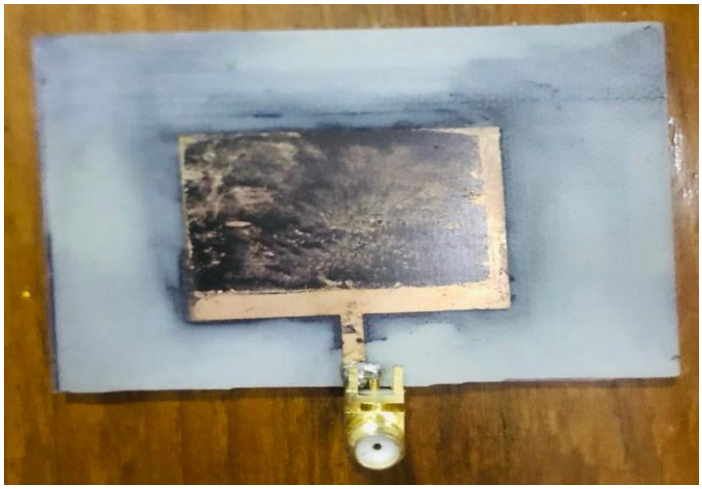

Figure (3.21) The fabricated CNT R-MPA (single)

3.5.1.2 (1×2) array R-MPA

The dimensions of array R-MPA are as follows:

Dimensions of each patch : width * length = (38 * 29) mm

Dimensions of feed line(50Ω) : width * length = (3 * 13.5) mm

Width of feed line (70 Ω) : 1.5 mm

Dimensions of substrate : width * length = (176.5 * 69) mm

A) Copper only

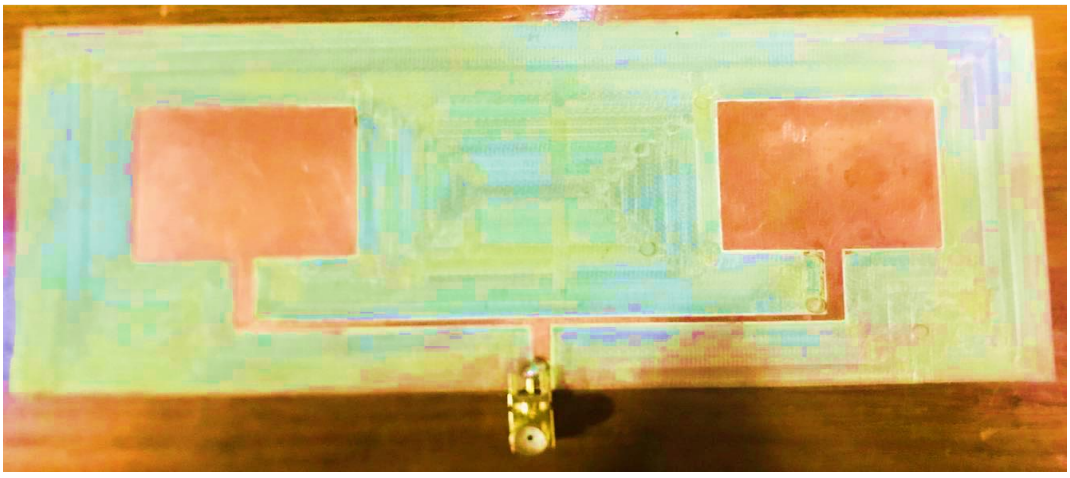

Figure (3.22) The fabricated R-MPA (array 1*2)

B) CNT with copper

Figure (3.23) The fabricated CNT R-MPA (array 1*2)

Chapter Four

Results and Discussion

4.1 **Introduction**

In this chapter, it will be mentioned the results of the basic characteristics of the designed and fabricated antennas in the previous chapter. After simulating the proposed designs by the port within CST program that it is connected to the antenna in a certain way (The port is known as the tool through which the design is simulated in the CST software), the analysis of several important results for the R-MPA was obtained , such as (Return loss, VSWR, directivity, gain, efficiency, and (2D, 3D) of the radiation pattern. In all of our designs, the return loss was less than -10 dB and VSWR from 1 to 2, this means that the antennas are performing well. The results of the different designs (single and array elements) were discussed and compared with each other to explain the differences between them.

4.2 Results of the designs

We designed six constructions of R-MPA, three by using copper and three by using CNT as we explained in Chapter 3. The simulation results that we have obtained through the CST software version 18.0 will be listed as follows:

4.2.1 Results of R-MPA of copper

In this section, we will include the results for three different designs by using copper.

a) Single element of R-MPA

After simulation of the antenna, the s parameter was -45.11 dB at 2.396 GH_z and VSWR was 1.011. The directivity was 6.87 dB_i and the gain was 3.64 dB at the resonant frequency. The radiation efficiency was -3.25dB. The S_{11}, VSWR and radiation pattern plots were shown in the figures (4.1) to (4.4).

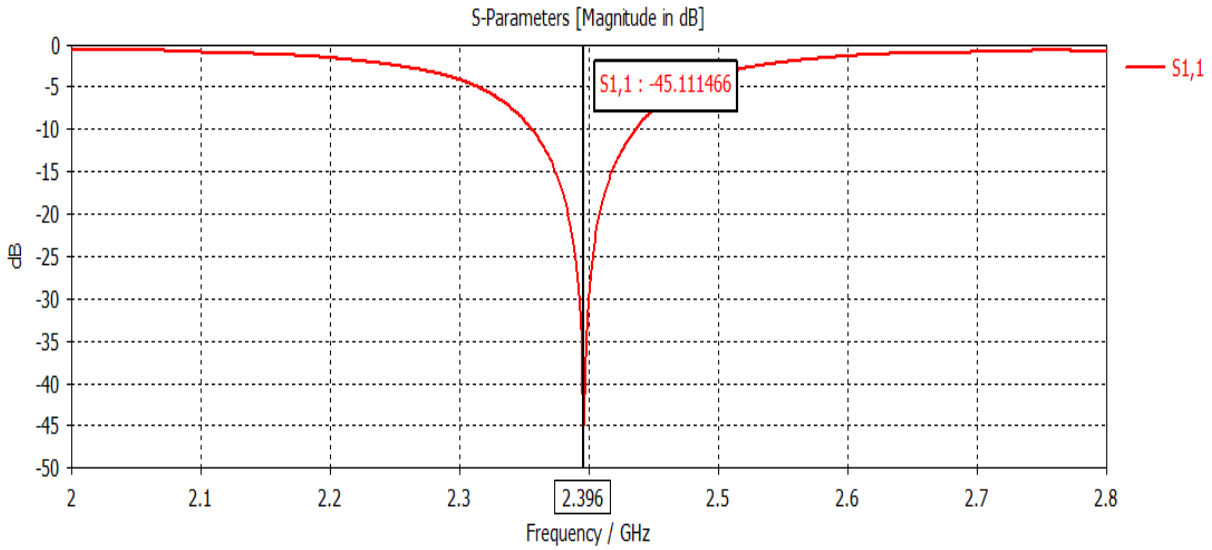

Figure (4.1) RL Vs. Frequency of single element copper R-MPA

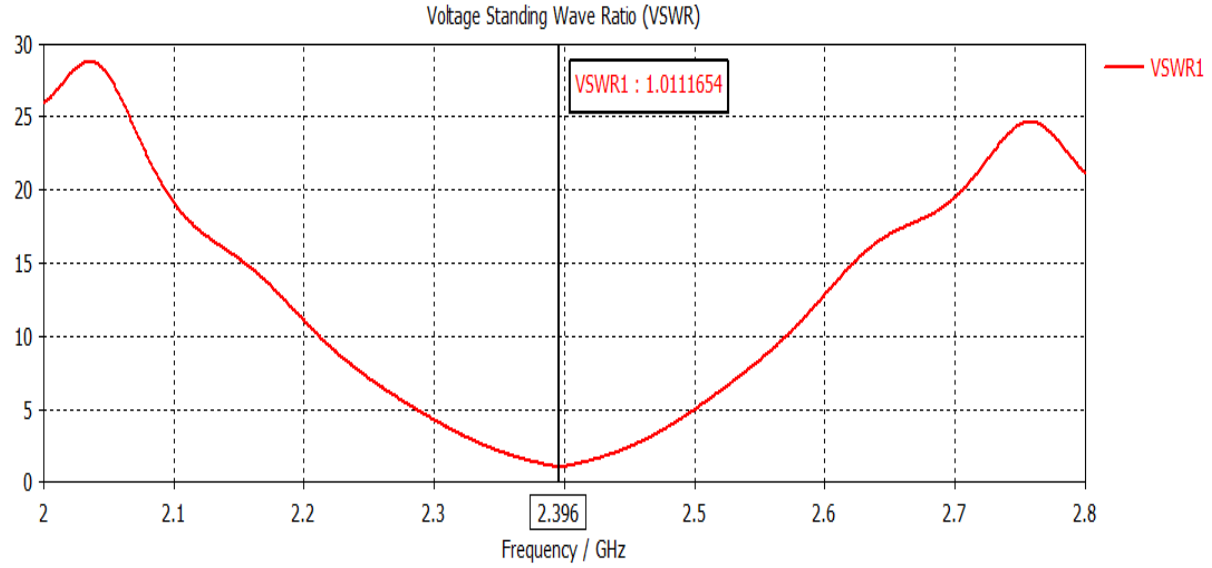

Figure (4.2) VSWR Vs Frequency of single copper R-MPA

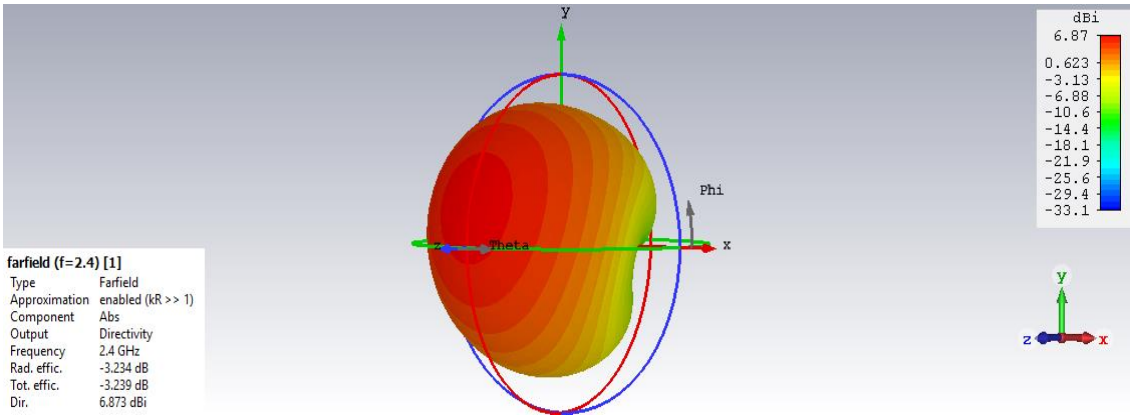

Figure (4.3) 3D Radiation Pattern of (single copper R-MPA)

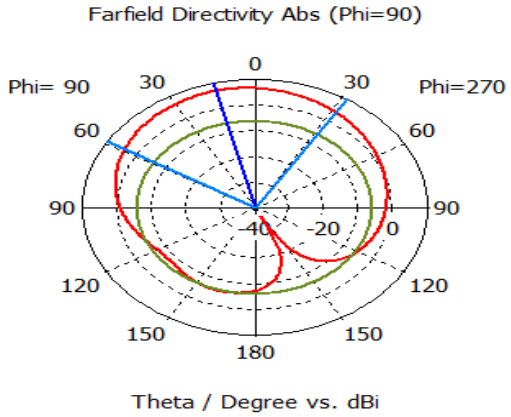

Figure (4.4) 2D Radiation Pattern of (single copper R-MPA)

Table (4.1) The important properties of single element copper R-MPA

Parameter	**Value**
Frequency	2.396 GH_z
S_{11}	-45.11 dB
VSWR	1.011
Directivity	6.87 dB_i
Gain	3.64 dB
Radiation efficiency	-3.25 dB

b)1*2 array of R-MPA

The RL was -10 at 2.4096 GHz and VSWR was 1.92. The directivity and gain were 10.5 dBi and 3.21 dB at the resonant frequency. The S_{11}, VSWR, efficiency, and radiation pattern plots were shown in the figures (4.5) to (4.8).The radiation efficiency was -5.16 dB.

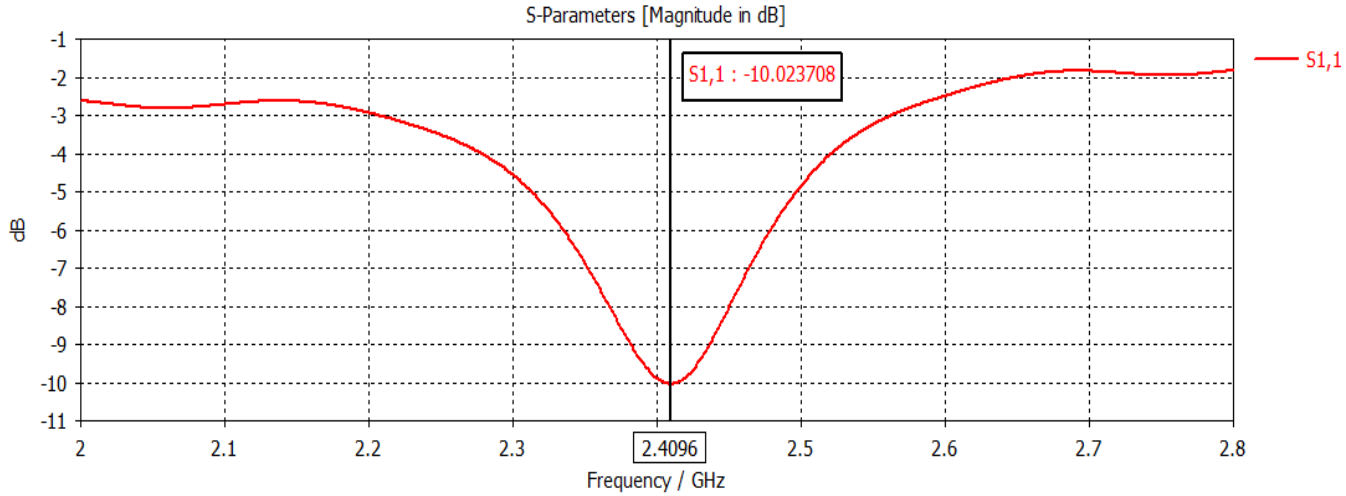

Fig (4.5) RL Vs. Frequency of 1×2 array copper R-MPA

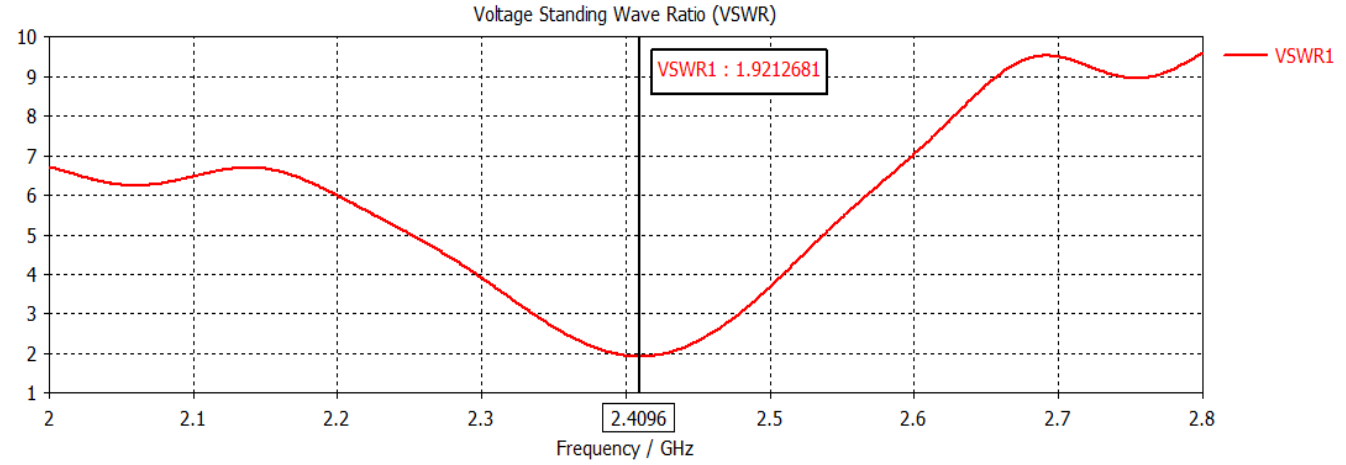

Figure (4.6) VSWR Vs Frequency of 1×2 array copper R-MPA

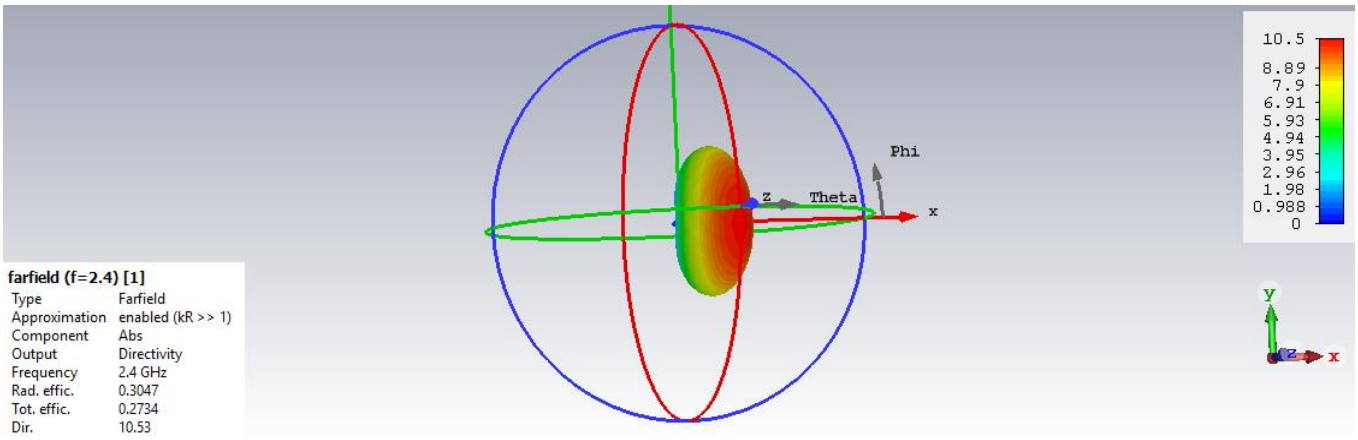

Figure (4.7) 3 D Radiation Pattern of (1*2 arrays copper R-MPA)

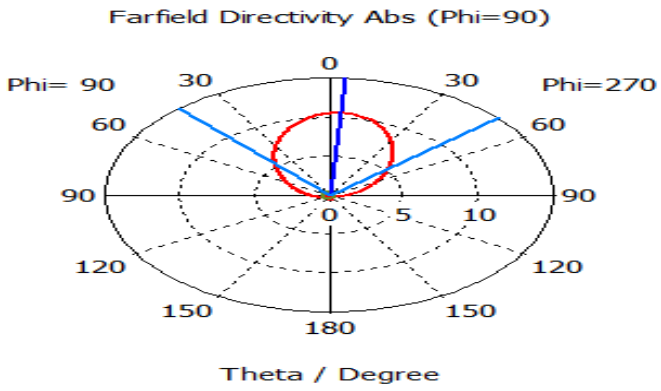

Figure (4.8) 2D Radiation Pattern of (1 * 2 array copper R-MPA)

Table (4.2) The simulated results of 1*2 array elements copper R-MPA

Parameter	**Value**
Frequency	2.4096 GHz
S_{11}	-10 dB
VSWR	1.92
Directivity	10.5 dB_i
Gain	3.21 dB
Radiation efficiency	-5.16 dB

c) 4×1 array of R-MPA

After simulation, the RL and VSWR were -47.56 dB and 1.0084 at 2.396 GHz. The directivity and gain were 7.56 dBi and 3.46 dB at the center frequency. The plots of the simulated results as shown in Figures (4.9) to (4.11). The radiation efficiency was -4.1 dB.

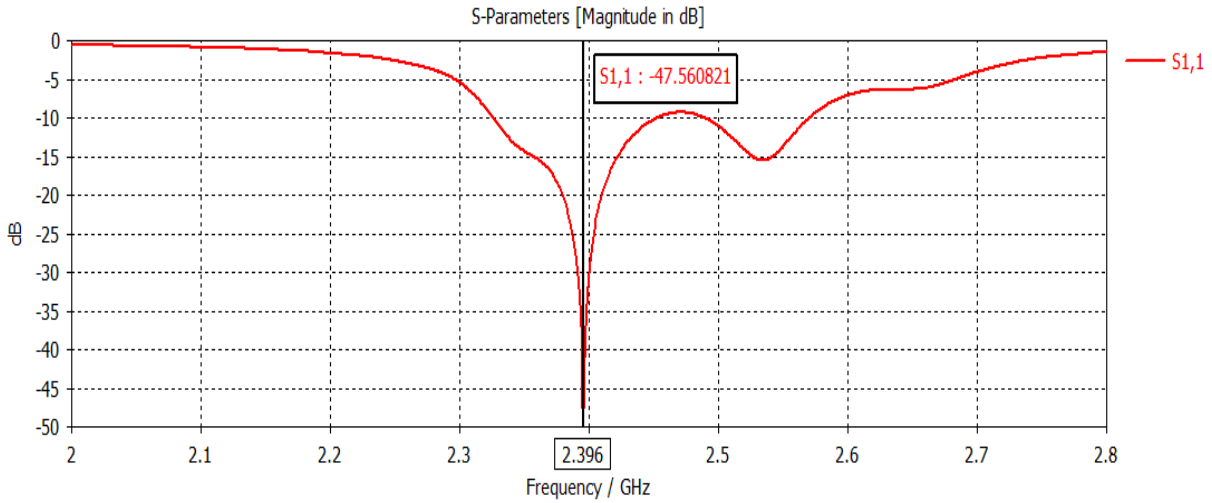

Figure (4.9) RL Vs. Frequency of 4×1 array copper R-MPA

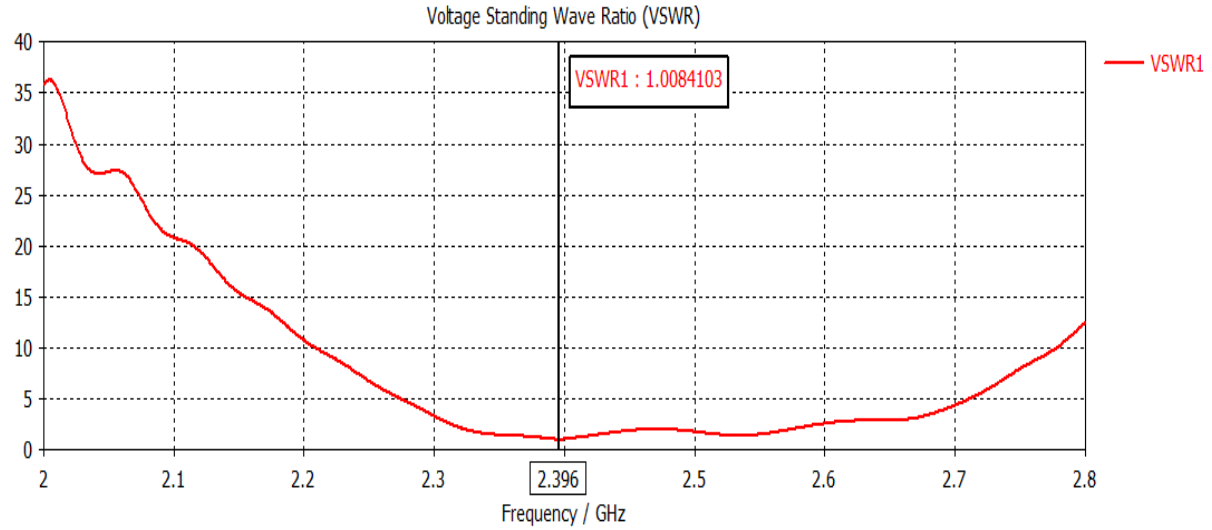

Figure (4.10) VSWR Vs Frequency of 4×1 array copper R-MPA

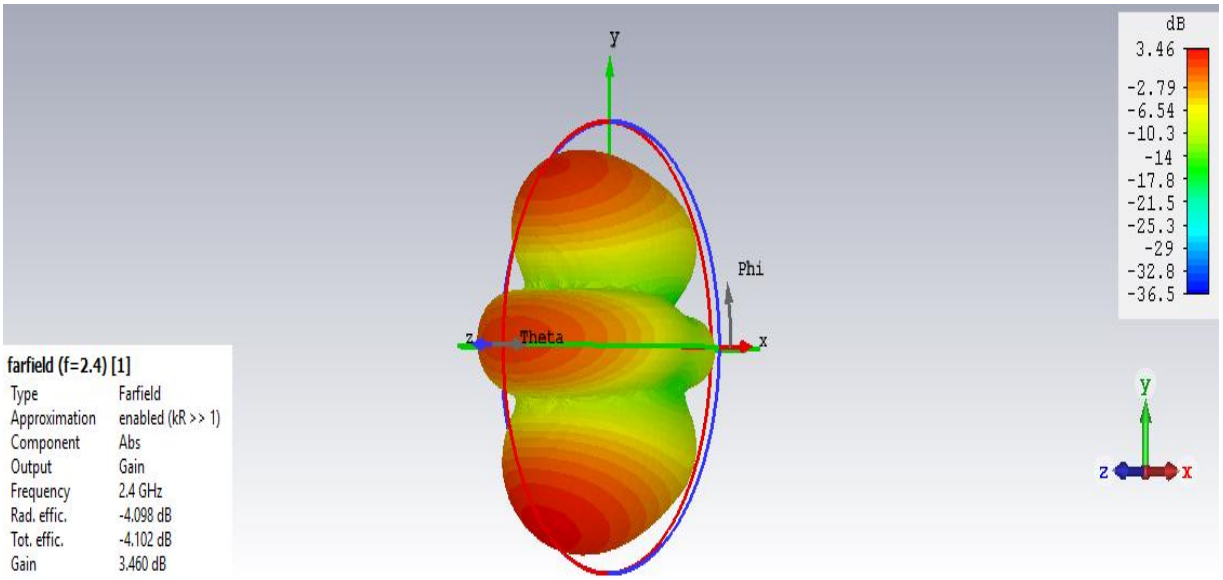

Figure (4.11) 3 D Radiation Pattern of (4*1 arrays copper R-MPA)

Table (4.3) The simulated results of 4×1 array elements copper R-MPA

Parameter	**Value**
Frequency	2.396 GHz
S_{11}	-47.56 dB
VSWR	1.0084
Directivity	7.56 dB_i
Gain	3.46 dB
Radiation efficiency	-4.1 dB

d) 1×4 array of R-MPA

Here the directivity and gain were improved. They were found to be 13.3 dB_i and 7.66 dB at the operating frequency. The s parameter was -16.57 dB at 2.3992 GH_z and VSWR was 1.34 . The results of the simulation were represented in the Figures (4.12) to (4.14).The radiation efficiency was -5.7 dB.

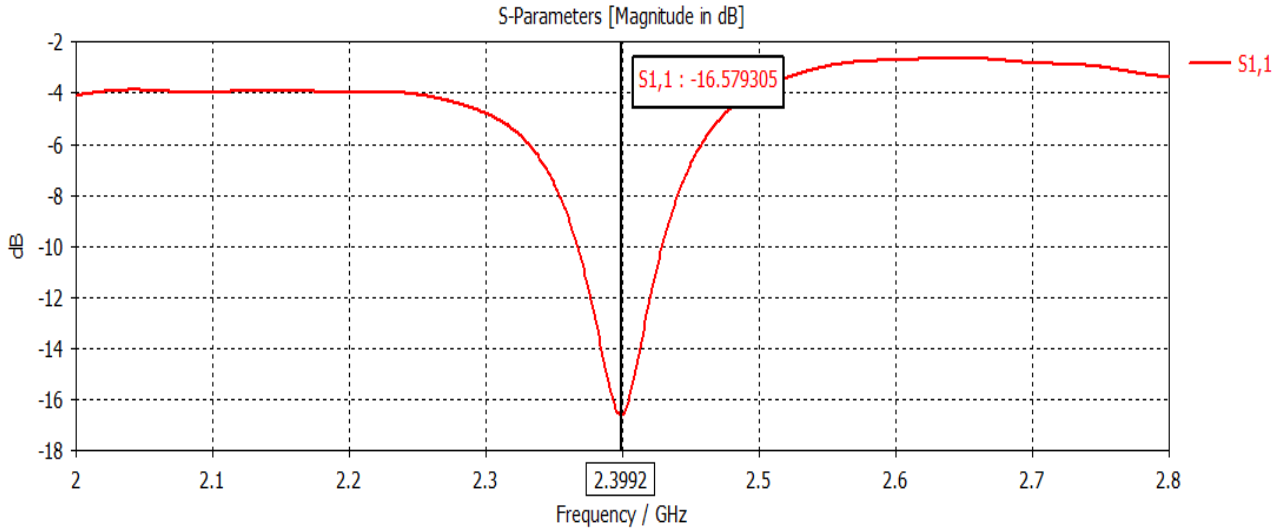

Figure (4.12) RL Vs. Frequency of 1×4 array copper R-MPA

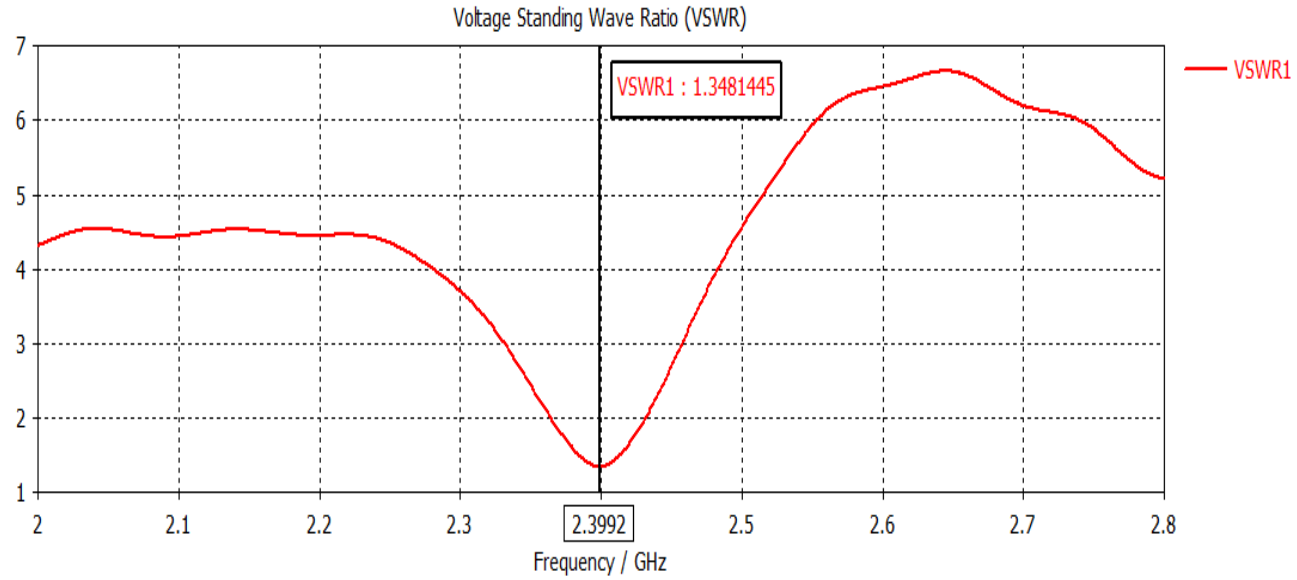

Figure (4.13) VSWR Vs Frequency of 1×4 array copper R-MPA

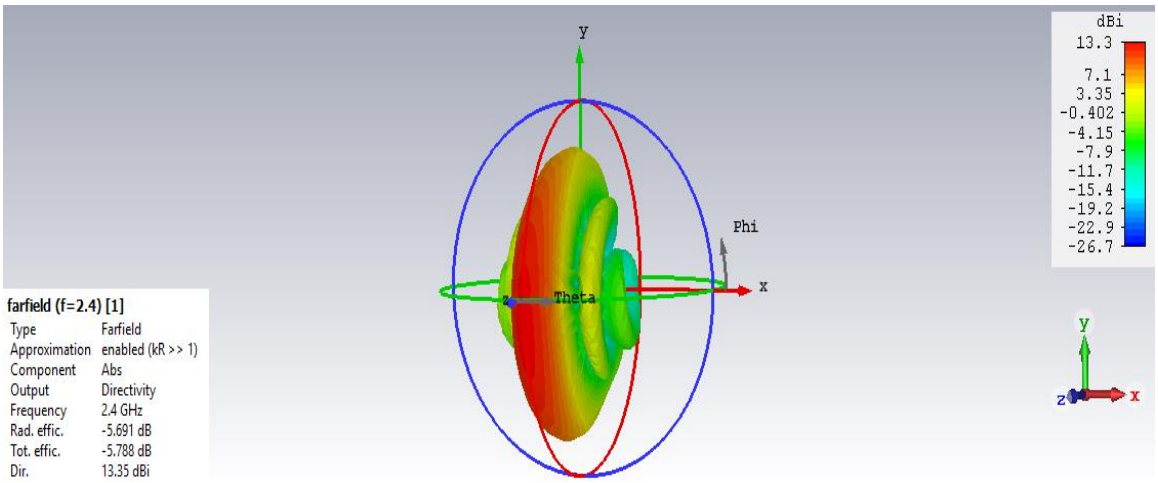

Figure (4.14) 3D Radiation Pattern of (1*4 arrays copper R-MPA)

Table (4.4) The simulated results of 1×4 array elements copper R-MPA

Parameter	**Value**
Frequency	2.3912 GH_z
S_{11}	-25.92 dB
VSWR	1.1
Directivity	13.3 dB_i
Gain	7.66 dB
Radiation efficiency	-5.7 dB

4.2.2 Results of R-MPA of CNT

In this section, the results for three different designs were geted by using CNT.

A) Single element of R-MPA

After simulation, the return loss and VSWR were -25.92 dB and 1.1 at 2.3912 GHz.

The directivity was 6.65 dBi and the gain was 2.62 dB at the resonant frequency. The figures (4.15) to (4.18) explain the diagrams of the simulated results. The radiation efficiency was -4.05 dB.

Table (4.5) The simulated results of single elements CNT R-MPA

Parameter	**Value**
Frequency	2.3992 GH_z
S_{11}	-16.57 dB
VSWR	1.34
Directivity	6.65 dBi
Gain	2.62 dB
Radiation efficiency	-4.05 dB

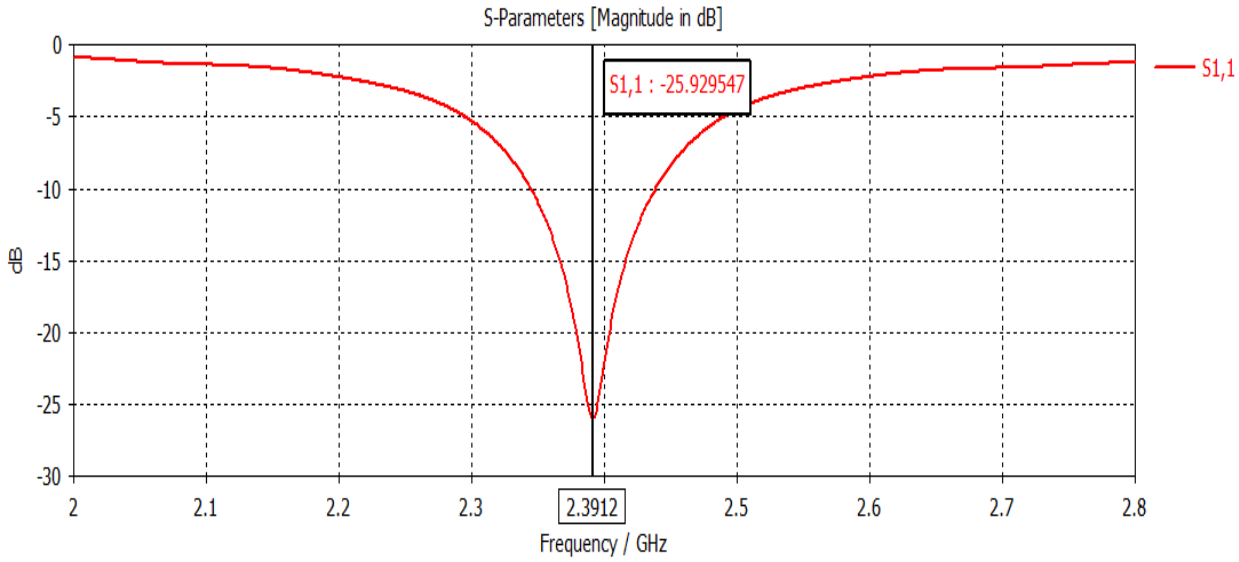

Figure (4.15) RL Vs. Frequency of single CNT R-MPA

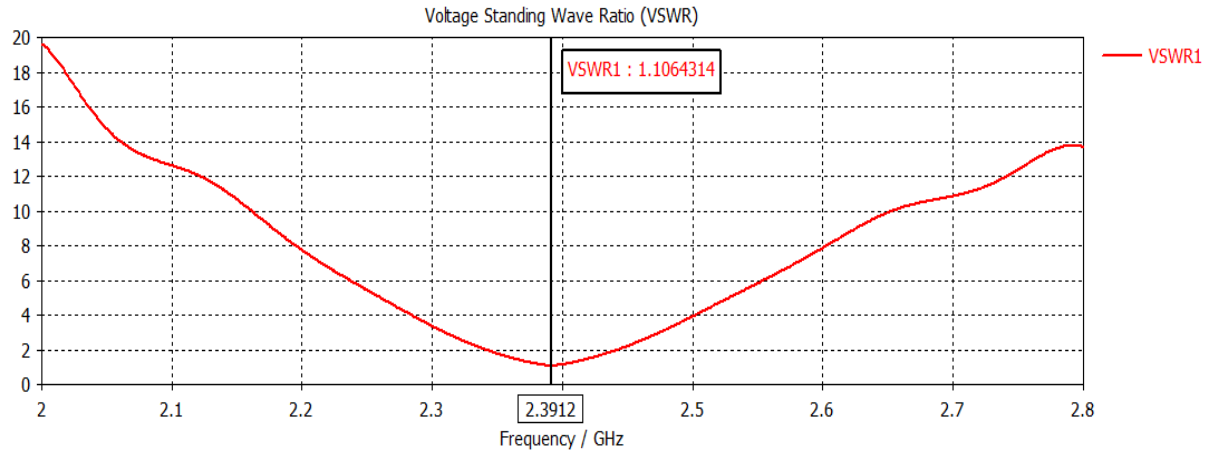

Figure (4.16) VSWR Vs Frequency of single CNT R-MPA

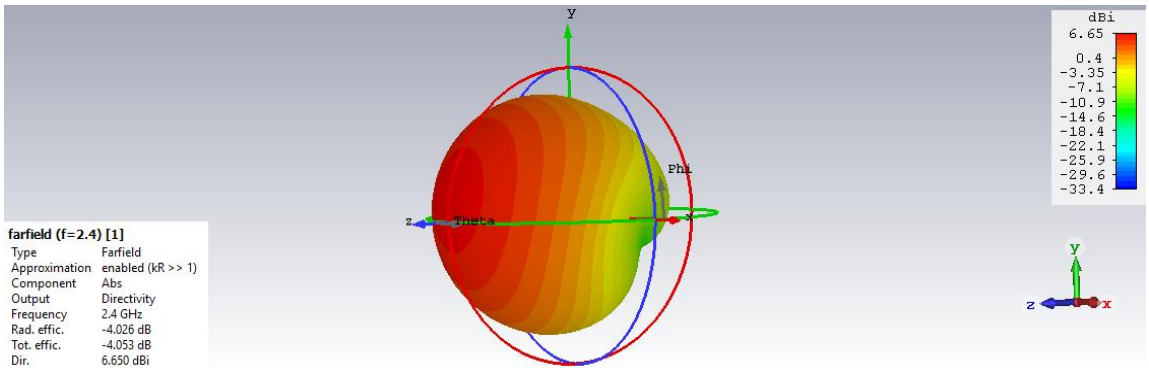

Figure (4.17) 3D Radiation Pattern of (single CNT R-MPA)

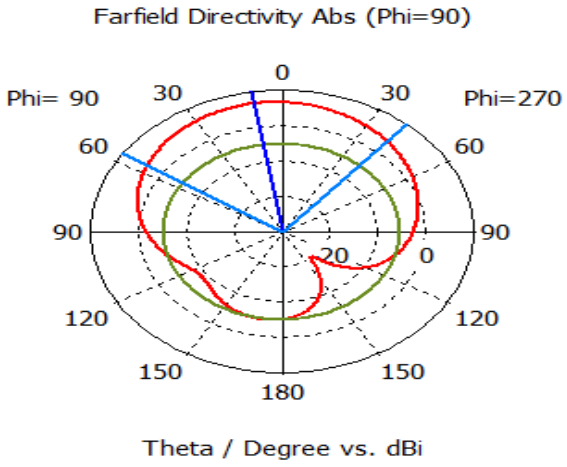

Figure (4.18) 2D Radiation Pattern of (single CNT R-MPA)

B) 4×1 array of R-MPA

S_{11} and VSWR of this design were -22.04 and 1.17 at 2.3976 GHz. The directivity and gain were 7.83 dBi and 3.2 dB at the resonant frequency. The simulated results in figures (4.19) to (4.21).The radiation efficiency was -4.63 dB.

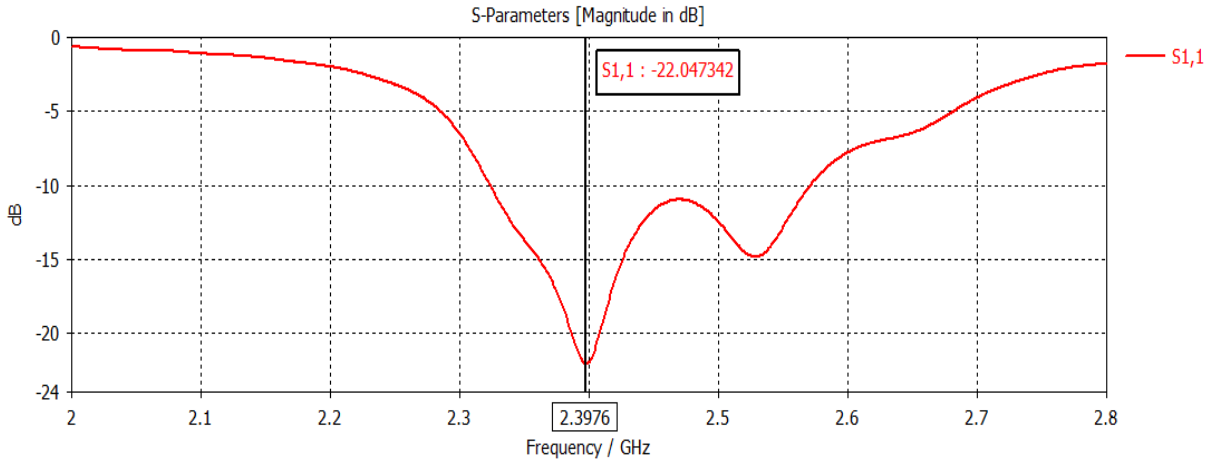

Figure (4.19) RL Vs. Frequency of 4×1 array CNT R-MPA

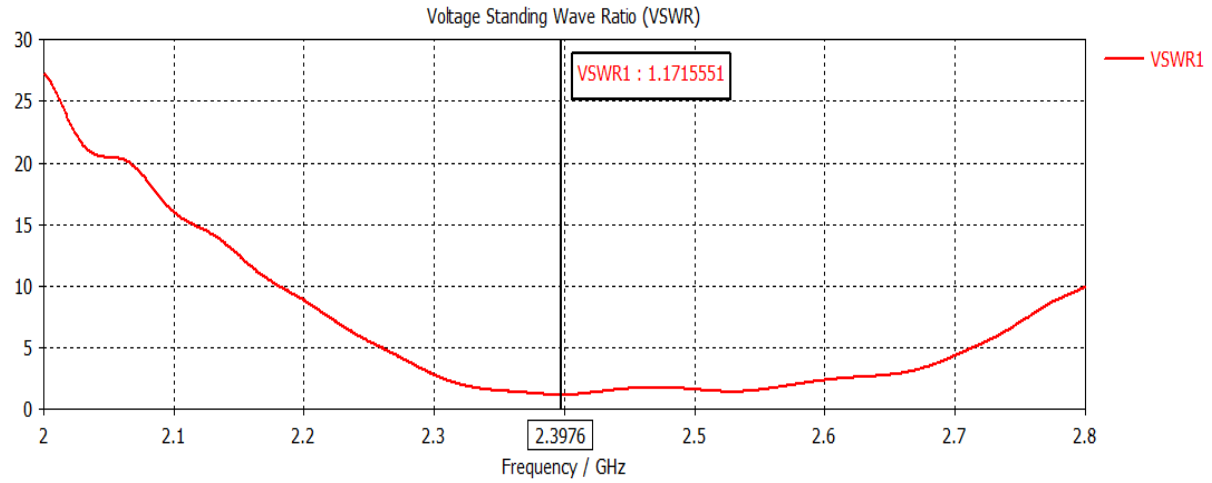

Figure (4.20) VSWR Vs Frequency of 4×1 array CNT R-MPA

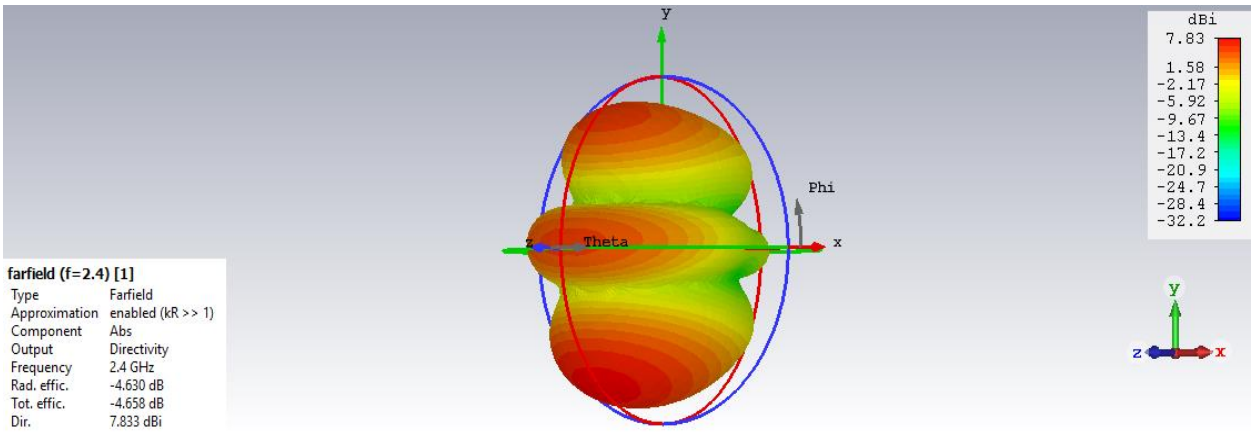

Figure (4.21) 3 D Radiation Pattern of (4*1 arrays CNT R-MPA)

Table (4.6) The simulated results of 4×1 array elements CNT R-MPA

Parameter	**Value**
Frequency	2.3976 GH_z
S_{11}	-22.04 dB
VSWR	1.17
Directivity	7.83 dBi
Gain	3. 2 dB
Radiation efficiency	-4.63 dB

C) 1×4 array of R-MPA

In this design, we got to the s parameter -12.93 at the frequency 2.4024 GHz and VSWR 1.58. The directivity 13.5 dBi and the gain 5.66 dB at the center frequency. The plots of S parameter, VSWR, gain and directivity in the figures (4.22) to (4.24).The radiation efficiency was -7.87 dB

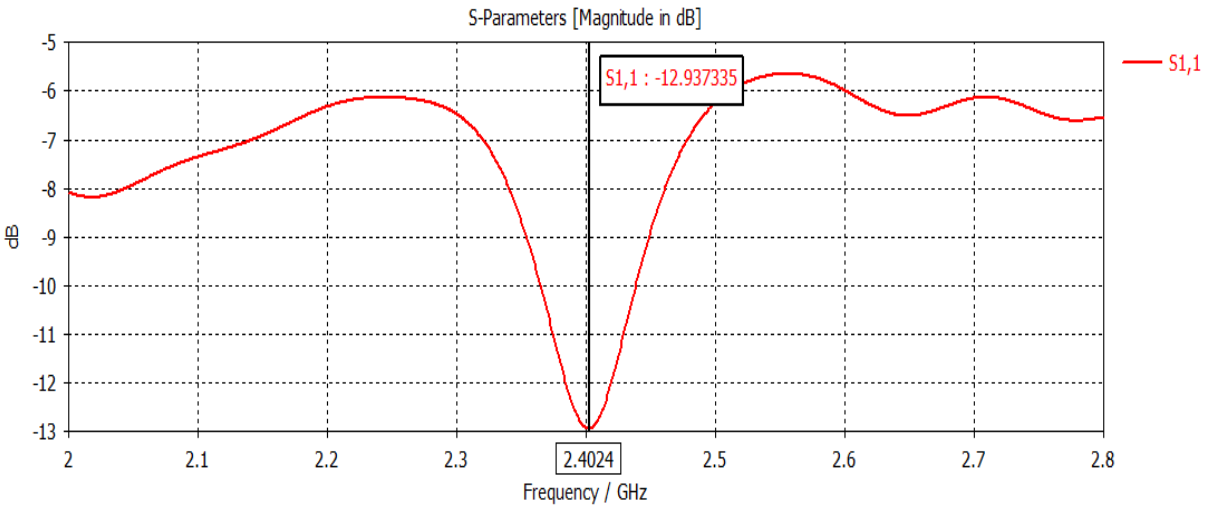

Figure (4.22) RL Vs. Frequency of 1×4 array CNT R-MPA

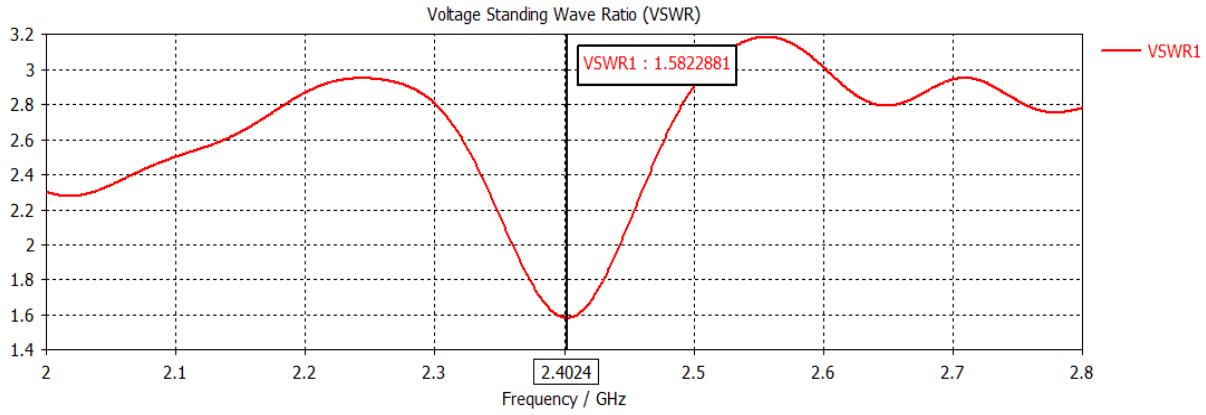

Figure (4.23) VSWR Vs Frequency of 1×4 array CNT R-MPA

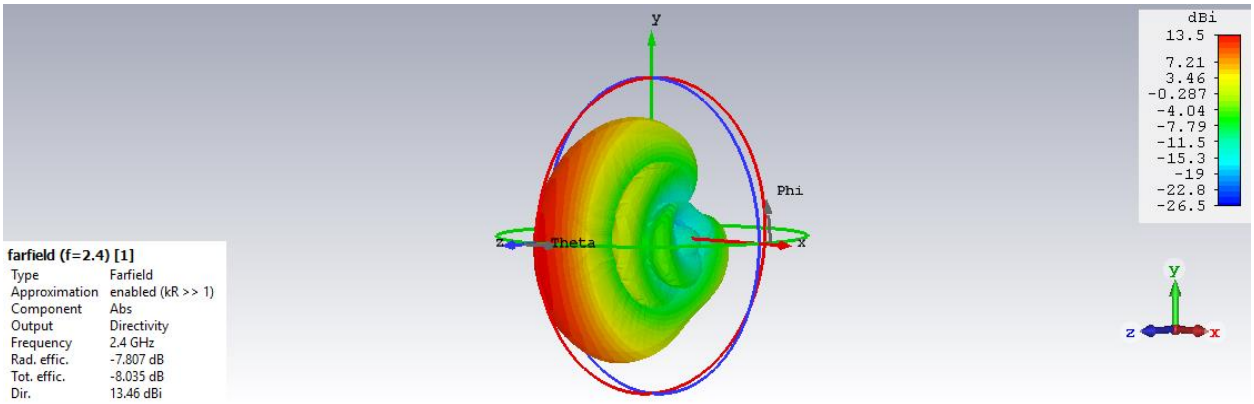

Figure (4.24) 3D Radiation Pattern of (1*4 arrays CNT R-MPA)

Table (4.7) The simulated results of 1×4 array elements CNT R-MPA

Parameter	**Value**
Frequency	2.4024 GHz
S_{11}	-12.93 dB
VSWR	1.58
Directivity	13.5 dBi
Gain	5.66 dB
Radiation efficiency	-7.87 dB

4.3 Comparation of results for all designs

In table (4.8), we wrote all simulation results for the proposed designs to make it easy to study. By studying these results, we found that the directivity of the single antenna was 6.87 dBi and the antenna array increased and became (7.56, 13) dB_i when using copper .Also, when using CNT, the directivity of the single antenna was 6.65 dB_i, and the antennas array became (7.83, 13.5) dB_i. The lowest value of return losses we obtained from the single antenna and the 4×1 array using copper, which amounted to (-45.11 , -47.56) respectively. The highest gain we got from a 1×4 array using copper was 7.66 dB. VSWR was very good, where its value has not exceeded 1.6 in all the designed antennas.

Table (4.8) all of the designs results

Elements	copper				Carbon nanotube			
	S_{11} (dB)	VSWR	Directivty (dBi)	Gain (dB)	S_{11}(dB)	VSWR	Directivity (dBi)	Gain (dB)
single	-45.11	1.01	6.87	3.64	-25.92	1.1	6.65	2.62
4×1 array	-47.56	1.008	7.56	3.46	-22.04	1.17	7.83	3.2
1×4 array	-16.57	1.34	13.3	7.66	-12.93	1.58	13.5	5.66

Figure (4.25) explain the plots of S_{11} parameters for the designed antennas by using copper at the operating frequency 2.4 GHz.S_{11} parameter of single element is -45.11 dB.It is -10 dB for 1×2 array elements. It is -47.56 dB for 4×1 array elements. It is -16.57 dB for 1×4 array elements. The lowest value of return loss was in the case of 4×1 array elements this means that this design is better than the other designs.

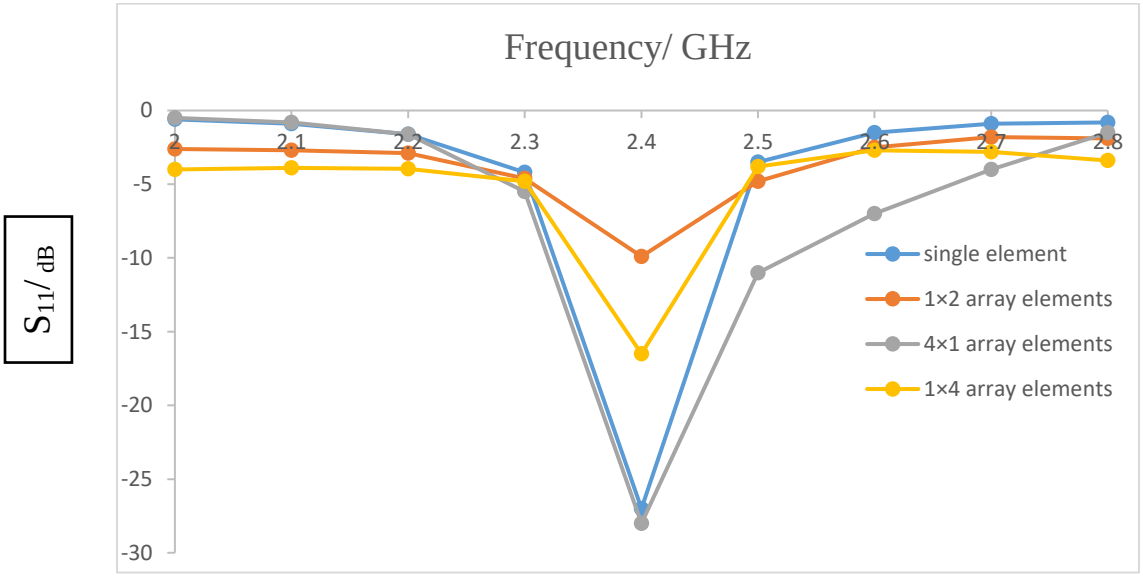

Fig (4.25) S_{11} vs Frequency of the designed R-MPA of copper

Figure (4.26) explains the plots of S_{11} parameters for the designed antennas by using CNT at the operating frequency 2.4 GHz.S_{11} parameter of single element is -25.92 dB. It is -22.04 dB for 4×1 array elements. It is -12.93 dB for 1×4 array elements. The lowest value of return loss was in the case of single element this means that this design is better than the other designs.

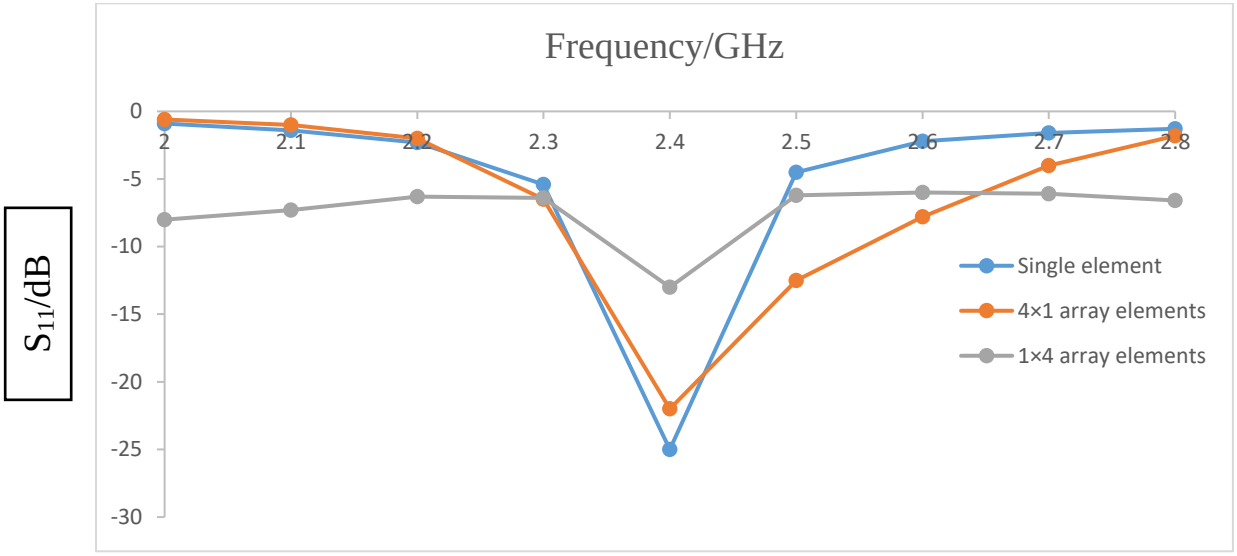

Fig (4.26) S_{11} vs Frequency of the designed R-MPA of CNT

4.4 Results of the fabricated antennas

1) Single element of R-MPA

A) Copper only

Testing the antenna shown in the figure (3.20) by using the Nano VNA device that measure the parameters of the antenna the most important is the frequency chart with the return loss (s-parameter) in dB as in the figure (4.27). The lowest return losses were - 6.54 dB at the operating frequency 2.408 GHz.

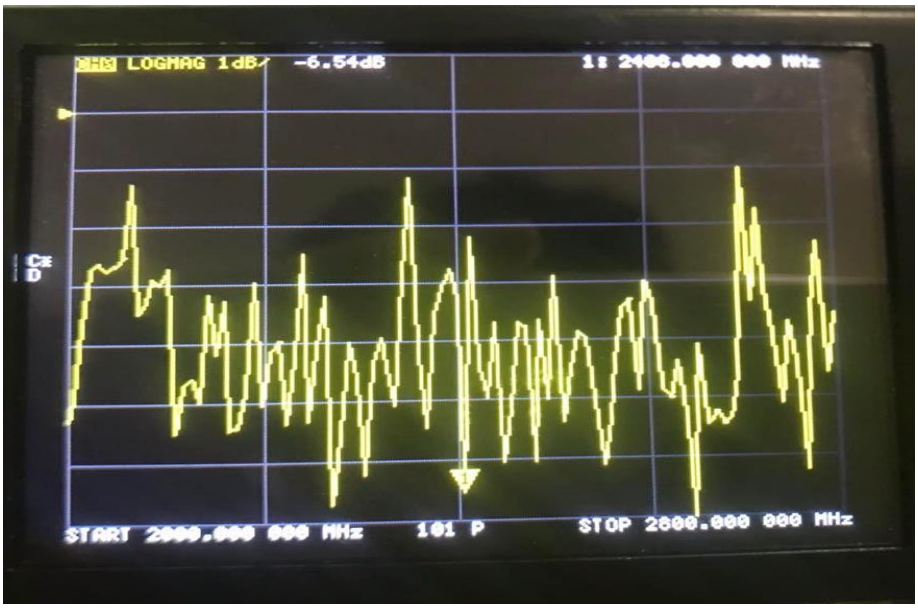

Figure (4.27) RL vs. Frequency of single R-MPA

B) CNT with copper

The diagram of the relationship between frequency and return losses is shown in the figure (4.28) and is measured by Nano VNA device. RL was -7.37 dB at 2.408 GHz.

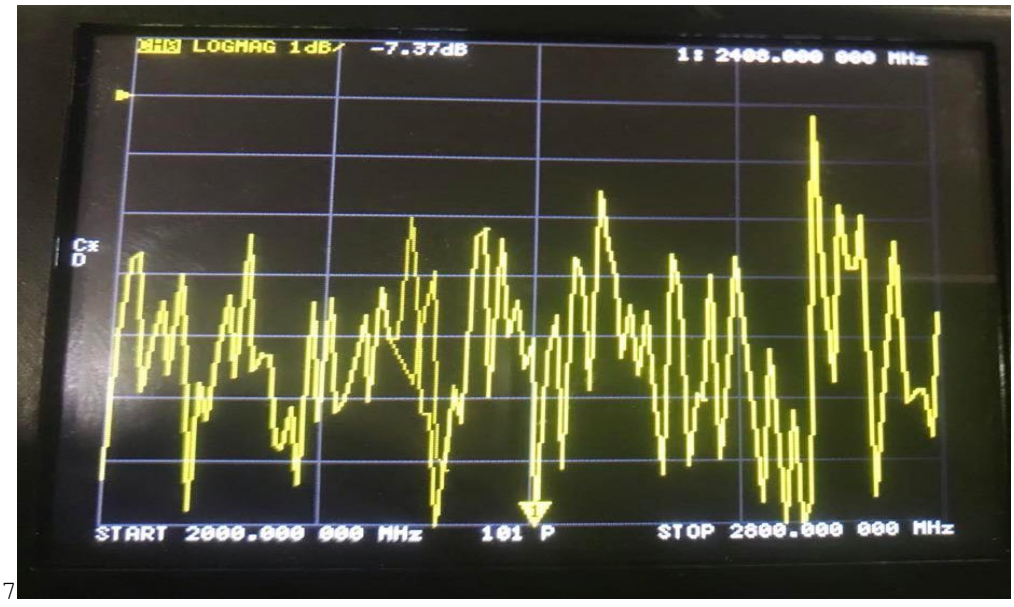

Figure (4.28) RL vs. Frequency of single CNT R-MPA

2) (1×2) array elements of R-MPA

A) Copper only

The measurement of return losses for the manufactured antenna is shown in Figure (4.29). RL was - 7.69 dB at 2.408 GH_z.

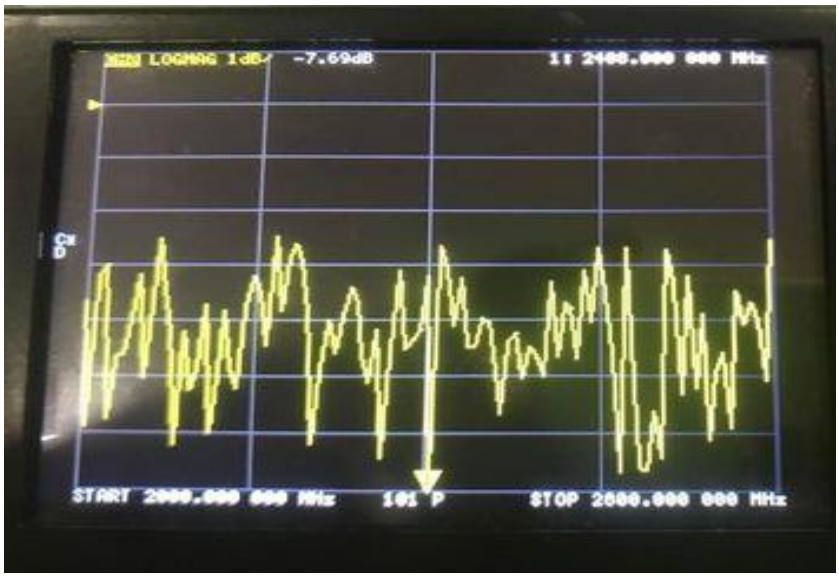

Figure (4.29) RL vs. Frequency of array (1*2) R-MPA

B) CNT with copper

Figure (4.30) shows that the operating frequency of the antenna was at the minimum value of s-parameter (-7 dB) where we notice through the figure (4.30) the resonant frequency is 2.408 GHz.

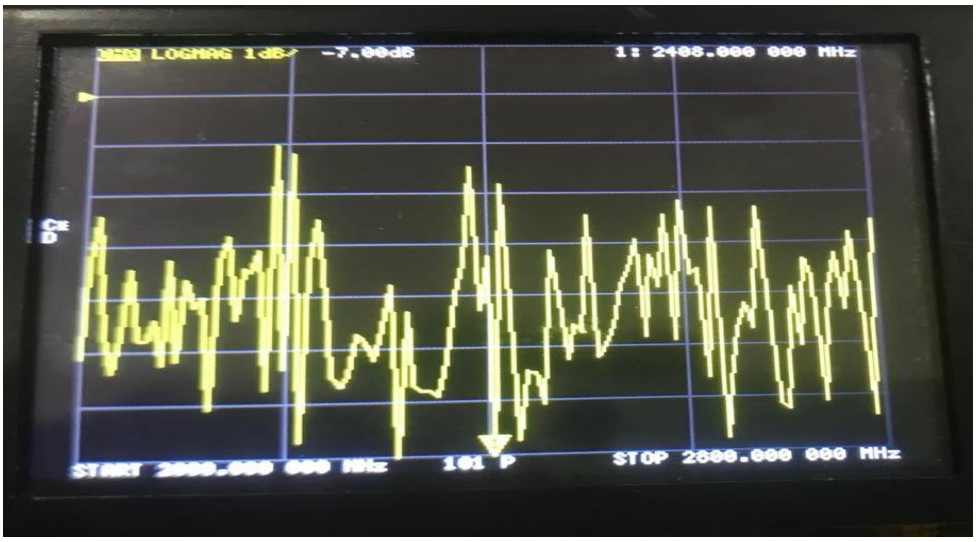

Figure (4.30) RL vs. Frequency of array (1*2) CNT R-MPA

4.5 Discussion of the experimented results

The values of return losses of the experimented results were not match to the simulated results. The s-parameter of the implemented antennas was more than -10 dB while it was always less than -10 dB of the designed antennas. This difference in results occurs due to the error rate in the manufacturing process.

Figure (4.31) explains the relationship diagram of the frequency and the s-parameter where contain two curves one representing the relationship for the simulated antennas and second representing the relationship for the fabricated antennas.

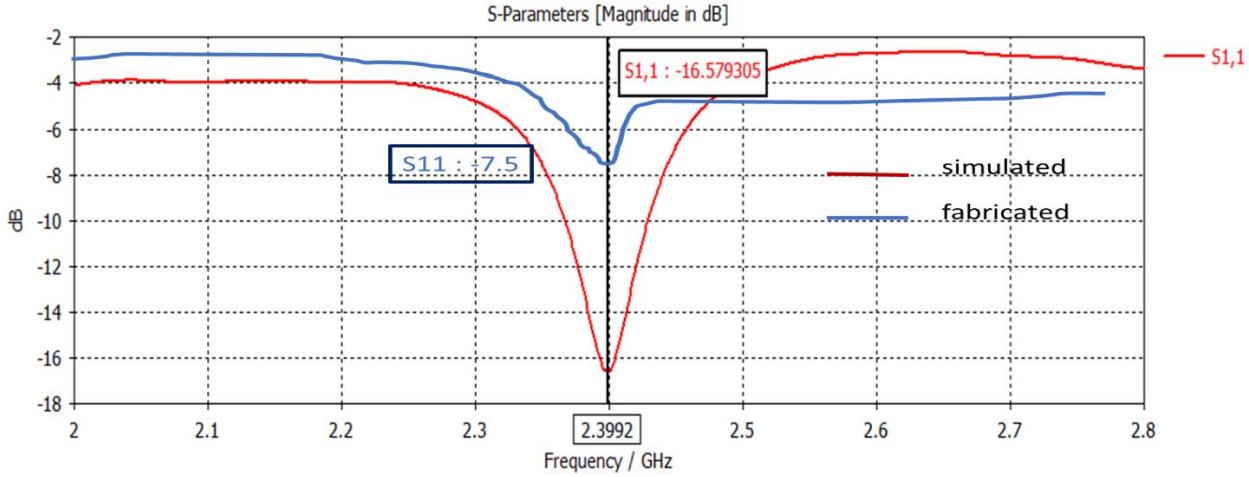

Figure (4.31) Comparing the return loss for the simulated and fabricated R-MPA

Chapter Five

Conclusions and Suggestion for Future work

5.1 Conclusion

In this search, R-MPA was designed and implemented based on copper and CNT. Single and array elements were used to form the antennas. The important characteristics of MPA have studied and discussed.

Several conclusions have been reached through this thesis, the most important of which are:

1) Through a result that mentioned in previous chapter, observed that when more than one patch is used to form an array of R-MPA, the general performance of the R-MPA will improve, as its gain and directivity increases. We also noticed that forming the array of MPA changing the properties for the same number of patches, since the corporate feeding is better than the series feeding, this applies in both copper and CNT for the same operating frequency and the same materials that make up the R-MPA.

2) When comparing the results of designed R-MPA using CNT with their counterparts designed using copper, found results were somewhat similar, only the difference is in the values of S_{11} parameter. It was found that the return losses in the case of copper are less than in the case of CNT.

3) The use of nanomaterials such as carbon nanotubes to design the patch antenna gives many advantages that were not found when using copper, such as the flexibility that makes CNT patch antenna enter into many applications such as medical and dealing with the human body. Also, the performance of the designed R-MPA from CNT can be improved by changing the properties of CNT by increasing its electrical

and magnetic conductivity, changing its thickness, or merging it with other chemical compounds, etc., while this is not possible in the designed R-MPA from copper.

4) The dimensions of the calculated R-MPA by the mathematical equations when they were entered into the CST program, they do not give very accurate results with the operating frequency to be operated, so we have to increase or decrease these dimensions by a very small amount to get a R-MPA that works within the frequency band allocated to it.

5.2 Future Work

1) In the future, the CNT R-MPA can be made using other substrate materials with the function to be performed. For example, to build a flexible CNT R-MPA for health care applications, such as wearable devices, and flexible electronics,etc., we must use a flexible substrate such as thermal paper.

2) Another nanomaterials can be used to design and to fabricate the R-MPA, such as silver nanoparticals, graphene, .. etc.

3) It is possible to make other shapes of the MPA, such as the circular shape, particularly in the case of attaching antenna to a mobile devices such as airplane.

References

[1] Fang, D. G. (2017). *Antenna theory and microstrip antennas*. CRC Press.

[2] Fatthi Alsager, A. (2011). Design and analysis of microstrip patch antenna arrays.

[3] Patel, B. D. (2013, April). Microstrip Patch Ante nna-A Historical Pe rspe ctive of the Developme nt. In *Conference on Advances in Communication and Control Systems (CAC2S 2013)* (pp. 445-449). Atlantis Press.

[4] Kant, R., & Dhubkarya, D. C. (2010). Design & Analysis of H-Shape Microstrip Patch Antenna. *Global Journal of Research in Engineering*, *10*(6).

[5] Patel, S. K., & Kosta, Y. P. (2011, December). E-shape microstrip patch antenna design for GPS application. In *2011 Nirma University International Conference on Engineering* (pp. 1-4). IEEE.

[6] Sandeep, B. S., & Kashyap, S. S. (2012). Design and simulation of microstrip patch array antenna for wireless communications at 2.4 GHz. *International Journal of Scientific & Engineering Research*, *3*(11), 1-5.

[7] Paul, L. C., & Sultan, N. (2013). Design, simulation and performance analysis of a line feed rectangular micro-strip patch antenna. *International Journal of Engineering Sciences & Emerging Technologies*, *4*(2), 117-126.

[8] Casu, G., Moraru, C., & Kovacs, A. (2014, May). Design and implementation of microstrip patch antenna array. In *2014 10th International Conference on Communications (COMM)* (pp. 1-4). IEEE

[9] Çalışkan, R., Gültekin, S. S., Uzer, D., & Dündar, Ö. (2015). A microstrip patch antenna design for breast cancer detection. *Procedia-Social and Behavioral Sciences*, *195*, 2905-2911.

[10] Midasala, V., & Siddaiah, P. (2016). Microstrip patch antenna array design to improve better gains. *Procedia computer science*, *85*, 401-409.

[11] Devi, K. C., Angadi, B., & Mahesh, H. M. (2017). Multiwalled carbon nanotube-based patch antenna for bandwidth enhancement. *Materials Science and Engineering: B*, *224*, 56-60.

[12] Dashti, M., & Carey, J. D. (2018). Graphene microstrip patch ultrawide band antennas for THz communications. *Advanced Functional Materials*, *28*(11), 1705925.

[13] Amram Bengio, E., Senic, D., Taylor, L. W., Headrick, R. J., King, M., Chen, P., ... & Pasquali, M. (2019). Carbon nanotube thin film patch antennas for wireless communications. *Applied Physics Letters*, *114*(20), 203102.

[14] Prakasam, V., LaxmiKanth, K. A., & Srinivasu, P. (2020, May). Design and simulation of circular microstrip patch antenna with line feed wireless communication application. In *2020 4th International Conference on Intelligent Computing and Control Systems (ICICCS)* (pp. 279-284). IEEE.

[15] Muhammad, A. Y. U., Yusuf, S., Adam, S. M., Man, K. L., Hahanov, V., Chumachenko, S., & Litvinova, E. (2021). *Design and Simulation of Microstrip Patch Array Antenna for Wireless Communication System* (No. 7041). EasyChair.

[16] Bajwa, H., Patra, P., Ikram, A. A., & Mirza, J. (2010, June). Nanostructured conformable patch antenna array. In *2010 International Conference on Information and Emerging Technologies* (pp. 1-4). IEEE.

[17] Waterhouse, R. (2003). *Microstrip Patch Antennas: A Designer's Guide: A Designer's Guide*. Springer Science & Business Media

[18] Garg, R., Bhartia, P., Bahl, I. J., & Ittipiboon, A. (2001). *Microstrip antenna design handbook*. Artech house.

[19] Shimu, N. J., & Ahmed, A. (2016, May). Design and performance analysis of rectangular microstrip patch antenna at 2.45 GHz. In *2016 5th International Conference on Informatics, Electronics and Vision (ICIEV)* (pp. 1062-1066). IEEE.

[20] Keller, S. D., Zaghloul, A. I., Shanov, V., Schulz, M. J., Mast, D., Alvarez, N. T., & Malik, R. (2019). Design and development of carbon nanotube antennas. In *Nanotube Superfiber Materials* (pp. 489-509). William Andrew Publishing.

[21] De, A., Chosh, C. K., & Bhattacherjee, A. K. (2016). Design and performance analysis of microstrip patch array antennas with different configurations. *International Journal of Future Generation Communication and Networking*, *9*(3), 97-110.

[22] Gupta, D., Duvey, A., & Agrawal, S. (2019). A Review: Microstrip Antenna.

[23] Alam, M. M., Sonchoy, M. M. R., & Goni, M. O. (2009, August). Design and performance analysis of microstrip array antenna. In *Progress In Electromagnetic Research Symposium Proceedings, Moscow, Russia* (pp. 18-21).

[24] Godara, L. C. (Ed.). (2018). *Handbook of antennas in wireless communications*. CRC press.

[25] Noor, A. (2012). *Design of microstrip patch antennas at 5.8 Ghz* (Master's thesis).

[26] Nakar, P. S. (2004). Design of a compact microstrip patch antenna for use in wireless/cellular devices.

[27] Balanis, C. A. (Ed.). (2011). *Modern antenna handbook*. John Wiley & Sons.

[28] Blake, L. V., & Long, M. W. (2009). Antennas: Fundamentals, Design. *Measurement*, *3*.

[29] Bansal, R. (Ed.). (2004). *Handbook of engineering electromagnetics*. CRC Press.

[30] Bancroft, R. (2019). *Microstrip and printed antenna design*. Institution of Engineering and Technology.

[31] Christodoulou, C. G., & Wahid, P. F. (2001). Fundamentals of antennas: concepts and applications.

[32] Pandey, A. (2019). *Practical microstrip and printed antenna design*. Artech House.

[33] Marhoon, H. M., & Qasem, N. (2020). Simulation and optimization of tuneable microstrip patch antenna for fifth-generation applications based on graphene. *International Journal of Electrical & Computer Engineering (2088-8708)*, *10*(5).

[34] Khanal, J. (2019). Design of Four Element Patch Array Antenna for IEEE 802.11 at 2.4 GHz.

[35] Milligan, T. A. (2005). *Modern antenna design*. John Wiley & Sons.

[36] Logothetidis, S. (Ed.). (2012). *Nanostructured materials and their applications*. Springer Science & Business Media.

[37] Jorio, Ado, Esko Kauppinen, and Abdou Hassanien. (2007). "Carbon-nanotube metrology." *Carbon Nanotubes*. Springer, Berlin, Heidelberg, 63-100.

[38] Garleff, J. K., Ulloa, J. M., Koenraad, P. M., & Bhushan, B. (2011). Scanning Probe Microscopy in Nanoscience and Nanotechnology 2.

[39] P. Moslemi, G. Askari, S. Mohajerzadeh, H. M. Sadeghi. (2012). , Application of Nanotechnology in High Frequency and Microwave Devices, Int. J. Theo. App. Nanotech. Vol. 1 (1), 134-140.

[40] Earp, B., Simpson, J., Phillips, J., Grbovic, D., Vidmar, S., McCarthy, J., & Luhrs, C. C. (2019). Electrically conductive CNT composites at loadings below theoretical percolation values. *Nanomaterials*, *9*(4), 491.

[41] M. S. Dresselhaus, G. Dresselhaus, R. Saito. (2000). , *Physics of Carbon Nanotubes*, Carbon 33 (7) , Vol. 33 (7) 883 -891.

[42] H. G. Chae, S. Kumar.(2006). , *Rigid Rod Polymeric Fibers*, J. Appl. Poly. Sci. 100 (1): 791–802.

[43] R. Brukh and S. Mitra. (2007). , *Kinetics of carbon nanotube oxidation*, J. Mater. Chem. 17, 619-623.

[44] K. S. Ibrahim. (2013).*Carbon nanotubes–properties and applications: a review*, Carbon let. 14(3), 131-144.

[45] J. A. Misewich, R. Martel, Ph. Avouris, J. C. Tsang, S. Heinze, J. Tersoff. (2003). , *Electrically Induced Optical Emission from a Carbon Nanotube FET*, Science 3000 (5620), 783-786.

[46] J. Chen, V. Perebeinos, M. Freitag, T. Marcus, F. James, Q. Fu, J. Liu, P. Avouris .(2005). , *Bright Infrared Emission from Electrically Induced Excitons in Carbon Nanotubes*, Science 310 (5751) 1171-1174.

[47] C. Yu, L. Shi, Z. Yao, D. Li, A. Majumdar .(2005). , *Thermal conductance and thermopower of an individual single-wall carbon nanotube*, Nano Lett, 5, 1842.

[48] J. Maultzsch, S. Reich, C. Thomsen, E. Dobardzic, I. Milosevic, M. Damnjanovic .(2002). , *Phonon dispersion of carbon nanotubes*. Solid State Commun, 121, 471.

[49] T. Maeda, C. Horie. (1999). *Phonon modes in single-wall nanotubes with a small diameter*. Physica B, 263-264, 479.

[50] Keller, S. D., Zaghloul, A. I., Shanov, V., Schulz, M. J., & Mast, D. B. (2013). Design considerations for a meshed carbon nanotube thread patch antenna. *IEEE Antennas and Wireless Propagation Letters*, *12*, 1192-1195.

[51] Chudasama, K. R., Anupkumar, P., & Ram, V. (2013). Design Of Carbon Nanotubes (CNT) Patch Antenna For WLAN Application.

[52] Javey, A., & Kong, J. (Eds.). (2009). *Carbon nanotube electronics*. Springer Science & Business Media.

[53] El-Sherbiny, S. G., Wageh, S., Elhalafawy, S. M., & Sharshar, A. A. (2013). Carbon nanotube antennas analysis and applications. *Advances in nano research*, *1*(1), 13.

[54] Singh, I., & Tripathi, V. S. (2011). Micro strip patch antenna and its applications: a survey. *Int. J. Comp. Tech. Appl*, *2*(5), 1595-1599.

[55] Ibrahim, R. A., Yagoub, M. C., & Habash, R. W. (2009, May). Microstrip patch antenna for RFID applications. In *2009 Canadian Conference on Electrical and Computer Engineering* (pp. 940-943). IEEE.

[56] Maulana, Y. Y., Wahyu, Y., Oktafiani, F., Saputra, Y. P., & Setiawan, A. (2016). Rectangular Patch Antenna Array for Radar Application. *TELKOMNIKA (Telecommunication Computing Electronics and Control)*, *14*(4), 1345-1350

[57] Aydın, E. A. (2021). A Novel Flexible Microstrip Patch Antenna with Different Conductive Materials For Telemedicine and Mobile Biomedical Imaging Systems.

[58] Bahl, I. J., Stuchly, S. S., & Stuchly, M. A. (1980, May). A microstrip antenna for medical applications. In *1980 IEEE MTT-S International Microwave symposium Digest* (pp. 358-360). IEEE.

[59] Dhariwal, S., Lamba, V. K., & Kumar, A. (2016). Simulation and performance analysis of carbon nano-materials based patch antennas. *Indian Journal of Science and Technology*, *9*(4), 1-8.

الخلاصة

نتيجة لتطور أنظمة الاتصالات اللاسلكية ومواكبة التقنيات الحديثة ، فإن ذلك يتطلب هوائيات يسهل تصنيعها وتتميز بأدائها العالي رغم صغر حجمها وقلة تكلفتها. لذلك ، تمت مناقشة هوائي الشريحة المايكروية (MPA) واستخدامه في العديد من التطبيقات التي تعتمد على الترددات العالية.

الهدف من هذه الأطروحة هو تصميم وتنفيذ MPA مستطيل يعتمد على النحاس وأنابيب الكربون النانوية (CNT) والذي يعمل ضمن نطاق الترددات الراديوية. تم تصميم MPA باستخدام الإصدار 18.0 من برنامج CST. أولاً ، تم استخدام النحاس كرقعة مشعة ، ثم استخدام CNT بدلاً من النحاس. في كلتا الحالتين ، تم استخدام نفس المواد لتصميم MPA. تم استخدام ركيزة من مثبطات اللهب 4 (FR4) مع $\varepsilon r = 4.3$ و $h =$ 1.6 مم وتم استخدام أرضية من النحاس. سماكة النحاس 0.035 مم وهي نفس سماكة أنابيب الكربون النانوية. تم تصميم ومحاكاة هوائي رقعة واحد بالإضافة إلى مجموعة من التصحيحات. تتكون المصفوفة من عنصرين وأربعة عناصر من التصحيحات. تم تصميمه باستخدام طريقتين مختلفتين ، خطوط تغذية متسلسلة ومتوازية. تم تحليل خصائص كل من هوائيات التصحيح النحاسية و CNT. كان تردد التشغيل لجميع الهوائيات المقترحة 2.4 جيجا هرتز ، والذي يستخدم للعديد من التطبيقات بما في ذلك Wi-Fi و Bluetooth. كانت خسارة العودة للهوائيات المصممة أقل من -10 ديسيبل ، بينما كانت نسبة موجة الجهد الدائمة (VSWR) بين 1 و 1.5. تم الحصول على خصائص MPA ومنها خسارة العودة ، VSWR ، الكسب ، الاتجاهية ، الكفاءة ، مخطط الإشعاع عند تردد الرنين.

اخيرا صنع العديد من هوائيات التصحيح microstrip باستخدام آلة CNC واختبارها تجريبياً باستخدام أداة Nano VNA. علاوة على ذلك ، تم إجراء مقارنة لمعرفة اختلاف الخصائص بين الهوائيات المصنعة والمحاكاة. بالإضافة إلى ذلك ، تم تصنيع واختبار هوائيات رقعة نحاسية مغلفة بـ CNT.

وزارة التعليم العالي والبحث العلمي

جامعة بابل

كلية الهندسة

قسم الهندسة الكهربائية

تصميم وتصنيع هوائي الشريحة المايكروية على أساس أنابيب الكربون النانوية

رسالة

مقدمة الى قسم الهندسة الكهربائية / كلية الهندسة

في جامعة بابل كجزء من متطلبات نيل درجة الماجستير

في علوم الهندسة/ الهندسة الكهربائية / الكترونيك صناعي

من قبل

سيف هلال زيدان نوري

اشراف

د. حيدر المؤمن

1444 هـ **2022 م**